

**ANALYSIS OF INTERMODULATION INTERFERENCE
TO THE INSTRUMENT LANDING SYSTEM**

by

YEANG, CHEN-PANG

B.S., National Taiwan University, Taipei, Taiwan

June 1992

Submitted to the Department of Electrical Engineering and Computer Science
in Partial Fulfillment of the Requirements for the Degree of

MASTER OF SCIENCE

at the

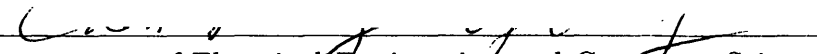
MASSACHUSETTS INSTITUTE OF TECHNOLOGY

January 1996

© Massachusetts Institute of Technology 1996

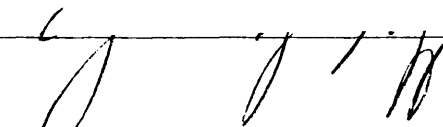
All rights reserved

Signature of Author



Department of Electrical Engineering and Computer Science

January 18, 1996

Certified by


Dr. Ying-Ching Eric Yang
Thesis Supervisor

Certified by


Professor Jin Au Kong
Thesis Supervisor

Accepted by

MASSACHUSETTS INSTITUTE
OF TECHNOLOGY


Frederic R. Morgenthaler
Chairman, Department Committee on Graduate Students

APR 11 1996

LIBRARIES



ANALYSIS OF INTERMODULATION INTERFERENCE TO THE INSTRUMENT LANDING SYSTEM

by

Yeang, Chen-Pang

Submitted to the Department of Electrical Engineering and Computer Science
on January 18, 1996 in partial fulfillment of the requirements for the degree of
Master of Science

ABSTRACT

This thesis provides a model that could quantitatively evaluate intermodulation interference for the localizer receivers of instrument landing system. In this model a receiver is divided into frequency selection stage, which selects the desirable RF signal and converts it to IF; and baseband stage, which retrieves course deviation from the localizer baseband waveform. Both stages are characterized by a set of parameters. The parameters are inverted by matching simulation results with experimental data for standard interference conditions. The model is then used to predict the course deviation current under any given interference environment.

Thesis Supervisor: Jin Au Kong

Title: Professor of Electrical Engineering

Thesis Supervisor: Ying-Ching Eric Yang

Title: Research Scientist, Research Laboratory of Electronics

Contents

Acknowledgment	7
List of Figures	11
List of Tables	13
Chapter 1 Introduction	15
1.1 Background	15
1.2 ILS Localizer Operating Principle	17
1.3 Types of Radio Interference to ILS	21
1.4 Overview of Problem and Methodology	23
Chapter 2 Generic Model for ILS Receiver	25
2.1 Localizer Receiver Architecture	25
2.2 Modeling of a Nonlinear Device	27
2.3 Modeling of Frequency Selection Stage	33
2.4 Modeling of Baseband Stage	44
Chapter 3 Model Synthesis	58
3.1 Experiments for ILS Receiver Interference	58
3.2 Model Synthesis-Inversion of Receiver Parameters	64
3.3 Inverted Receivers and Threshold Curves	69

Chapter 4 Simulation Results	74
4.1 Designing Future Receivers	74
4.2 Pure-Carrier Intermodulation Interference	78
4.3 Calculation of Course Deviation Current	81
Chapter 5 Conclusion	83
Reference	85

Acknowledgment

I wish to express my appreciation to my advisor Professor J. A. Kong, who provides me the chance to embark this study. His enthusiasm and kindness encourages the author of this thesis in many aspects.

I am deeply indebted to my research mentor, Dr. Eric Y. Yang. He gave me a lot of very precious guides and suggestions from shaping research scheme to conducting detailed theorization and simulation as well as writing a technical text. In a sense I am enlightened by him. I am also grateful to Dr. Robert T. Shin and Dr. A. Jordan for their direction on me to the methodology of scientific research.

I wish to thank Mr. Yan Zhang, my research partner. Some of the important ideas in this thesis were initiated by him. His warmth and diligence prove him a best research partner. I also wish to thank my senior Mr. Chih-Chien Hsu. He gave me a lot of help in familiarity with computers. My senior Shih-En Shih and my friend Tza-Jing Gung were the ones I can always count on. I would also like to thank them for their spiritual support. I am very fortunate to be surround with excellent persons in Professor Kong's group, Dr. Kung-Hau Ding, Dr. Jean-Claude Souyris, Dr. Joel Johnson, Mr. Jung Yan, other colleagues and our secretary Ms. Kit-Wah Lai.

Finally I wish to thank my parents for their support all these years.

“ You don’t want to become Buddha, nor do you want to learn alchemy ”

Said the Master, “ Then the only thing I can teach you is Magic ”

“ Gee! ”, the Monkey starts to contemplate

“ I heard his 108 Varieties are pretty fantastic, can I try them ? ”

—- Monkey King

List of Figures

1.1	Instrument Landing System	19
1.2	ILS operating principle	20
2.1	ILS receiver configuration	26
2.2	Typical nonlinear input/output relationship	29
2.3	RF-section block diagram	34
2.4	Block diagram of a balanced mixer	37
2.5	Sixth-order Chebyshev filter	40
2.6	IF-section block diagram	40
2.7a	Configuration of AGC	43
2.7b	Procedures for AGC simulation	43
2.8a	FM power spectrum. The 20-dB bandwidth is 64 KHz	47
2.8b	Modeled FM power spectrum	47
2.9	Envelope detector circuit	50
2.10	IF and baseband noise spectrum (one side)	54
2.11	CDI output based on simulated and approximated envelope detector	57
2.12	CDI mean and standard deviation	57
3.1	Experimental setup for ILS B1-interference tests	59

3.2	FAA intermodulation threshold test results	62
3.3	Parameter inversion procedures	68
3.4	Inverted AAM RF pre-filter response	71
3.5	Inverted ITU RF pre-filter response	71
3.6	AAM two-frequency B1 curves	72
3.7	AAM three-frequency B1 curves	72
3.8	ITU two-frequency B1 curves	73
3.9	ITU three-frequency B1 curves	73
4.1	Inverted ICAO RF pre-filter response	76
4.2	ICAO two-frequency B1 curves	77
4.3	ICAO three-frequency B1 curves	77
4.4	Comparison of pure-carrier interference with FM interference: AAM model	79
4.5	Comparison of pure-carrier interference with FM interference: ITU model	79
4.6	Comparison of pure-carrier interference with FM interference: ICAO model	80
4.7	Specification of over-threshold, threshold and under-threshold conditions	81
4.8	CDI distribution: over-threshold	82
4.9	CDI distribution: threshold	82
4.10	CDI distribution: under-threshold	82

List of Tables

2.1	Simulated CDI for zero-noise conditions	56
3.1	Intermodulation frequencies (two frequencies)	70
3.2	Intermodulation frequencies (three frequencies)	70
3.3	Inverted receiver parameters	70
4.1	Inverted ICAO receiver parameters	76

Chapter 1

Introduction

1.1 BACKGROUND

For the past few decades, Instrument Landing System (ILS) has been used to provide precision landing aid for aircraft during the period of low visibility. The operation of instrument landing system depends on the communication of radio signals between ground-based transmitters and airborne receivers. The ILS radio signals provide information of the aircraft course deviation, height and distance from the landing spot. The messages retrieved from airborne sensor can be fed into the aircraft control system. Newly developed landing systems such as Microwave Landing System (MLS) and Global Positioning System (GPS) adopt different spectrum regions, system architecture or coding characteristics; but they also rely on propagation of EM waves to get information of the airplane.

Since its invention ILS has worked well for the airports around the world without serious incidence. However, increasingly hostile radio environment around the airports due to urban development has gradually threatened its performance. Larger number of airport within a region makes it difficult to find ILS frequencies for different runways without running into interfering with other radio navigation systems. Buildings construction around the airport increases the opportunity of multipath interference to ILS radio signals. In addition, growth of FM stations, Industrial-Scientific-Medical equipment (ISM) and other instruments which radiate frequencies adjacent to ILS spectrum region also aggravates interference potential. The affore mentioned new systems is under consideration but the civil aviation authorities also made significant effort to alleviate those existing problems. The new landing systems utilizing different frequency band and signal processing schemes, such as MLS and GPS, have been developed. Before the transition to new systems has completed, however, the principal system is still ILS. Therefore the evaluation and improvement of ILS interference immunity are very important.

An appropriate way to conduct the evaluation of automatic landing system is to do statistical simulation on the landing process under realistic radio environment. The statistical parameters obtained from simulation such as failure rate are the basis for performance evaluation. In order to complete this simulation a theoretical ILS receiver model studying at the effect of radio interference is necessary. It is known that ILS interference comes from different types of mechanisms. In this thesis we choose intermodulation interference to be the target of analysis. It is because the spectrum range of a specific ILS subsystem: localizer (108.1 MHz to 111.95 MHz) is very close to FM broadcast band (88.1 MHz to 107.9 MHz), FM power (1 to 100 KW) is much larger than localizer power (15W), and therefore FM broadcasting signals are capable of driving the receiver into nonlinear region to generate intermodulation components. The frequencies of low-order intermodulation components, which often possess larger power, are close to localizer band. Apparently FM intermodulation interference is a non-negligible problem for ILS localizer.

The purpose of this thesis is to present an analysis of intermodulation interference on ILS localizer receiver. A generic model based on ILS circuit configuration is developed to cover the general population of receivers in service. This model contains the frequency selection part which include sections from RF to IF, and baseband signal processing part which include sections from IF envelope detector to output. The output error as a function of interfering frequencies is simulated and compared with empirical results. In order to invert appropriate receiver parameters an optimization technique is adopted to fit experimental results. This generic model is then used to extrapolate system response in other radio environments.

1.2 ILS LOCALIZER OPERATING PRINCIPLE

Instrument landing system (ILS) consists of three subsystems: localizer transmitter for azimuth guidance, glide slope transmitter for vertical guidance and marker beacons or distance measuring equipment (DME) for distance-to-threshold guidance. The placement of ground systems and rough sketch of operating principles are indicated in Figure 1.1. The localizer frequencies span from 108.1 to 111.95 MHz. There are altogether 40 channels, allocated at odd 100 KHz and 50 KHz frequencies. The glide slope frequencies span from 328.6 to 335 MHz. The DME frequencies span from 960 to 1215 MHz. These three components are tied together, so there are 40 channels in glide slope and DME as well [10].

ILS localizer provides the measure of azimuth deviation of airplane from the runway center line. Its operating principle is illustrated in Figure 1.2. The ground system contains a set of transmitting antenna arrays near the end of runway. The transmitted signal has two components, which are 90 Hz and 150 Hz respectively, amplitude-modulated with localizer carrier frequency f_{loc} . The arrays are arranged such that the beam patterns for the two modulated signals point to different sides of the runway and are symmetric. Thus along the runway centerline, their signal

strength are equal. The field strengths in front of both antenna sets are of the same power and modulation index, i.e. $A_{loc}^{Tx}[1 + m \cos(2\pi \cdot 90t)] \cos(2\pi f_{loc}t)$ and $A_{loc}^{Tx}[1 + m \cos(2\pi \cdot 150t)] \cos(2\pi f_{loc}t)$. The airborne receiver tuned at same localizer channel f_{loc} detects a combination of 90 Hz and 150 Hz signals $A_{loc}^{Rx}[1 + m_{90} \cos(2\pi \cdot 90t) + m_{150} \cos(2\pi \cdot 150t)] \cos(2\pi f_{loc}t)$. As indicated in Figure 1.2, m_{90} and m_{150} are functions of aircraft angular deviation θ . The way they are related to θ depends on the shape of antenna beam pattern. With a narrow range of θ , usually between -2° and 2° , the difference in depth of modulation (DDM), $m_{90}(\theta) - m_{150}(\theta)$, is approximately proportional to θ . The numerical bound of modulation indices m_{90} and m_{150} can be calculated on the basis of localizer antenna beam pattern and modulation index of transmitted AM. Within the two-degree range the modulation indices are bounded within 0.2 ± 0.0775 . A localizer receiver outputs $+150\mu\text{A}$ course deviation current when the angular deviation is $+2^\circ$, and $-150\mu\text{A}$ current when the angular deviation is -2° . The function of localizer receiver is to retrieve DDM from the input signal

$$A_{loc}^{Rx}[1 + m_{90} \cos(2\pi \cdot 90t) + m_{150} \cos(2\pi \cdot 150t)] \cos(2\pi f_{loc}t)$$

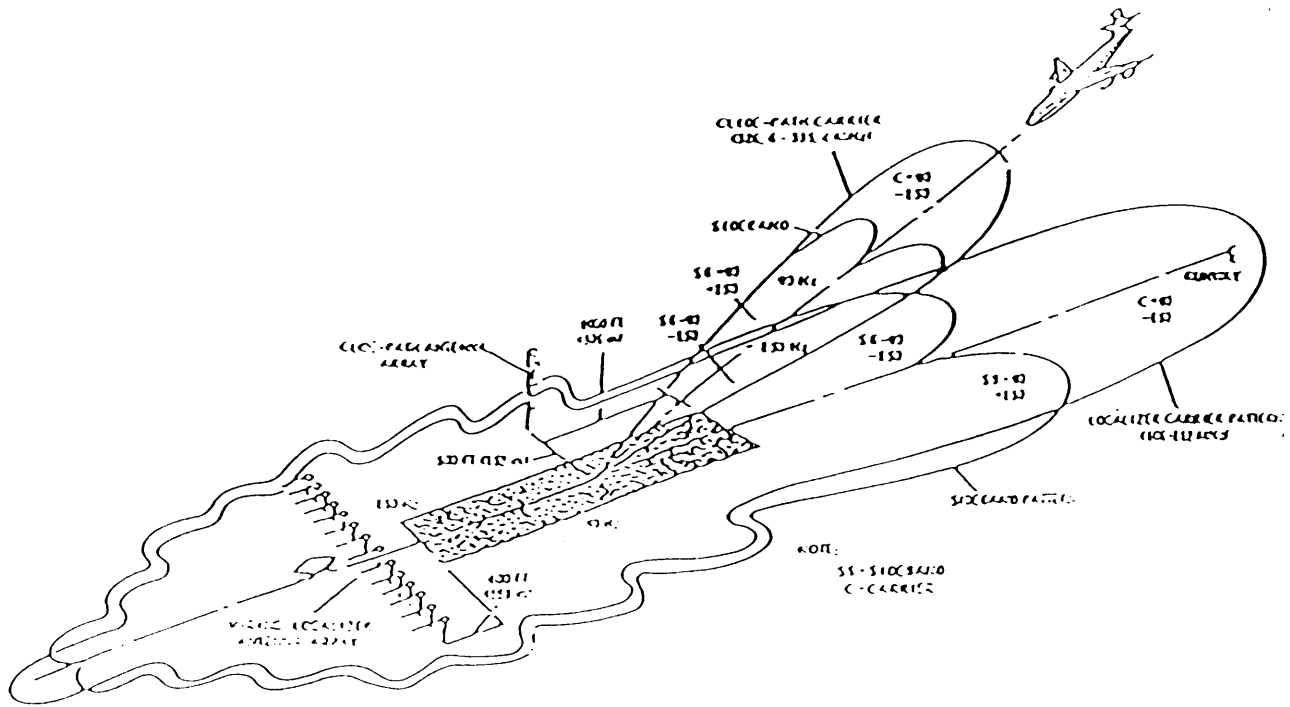
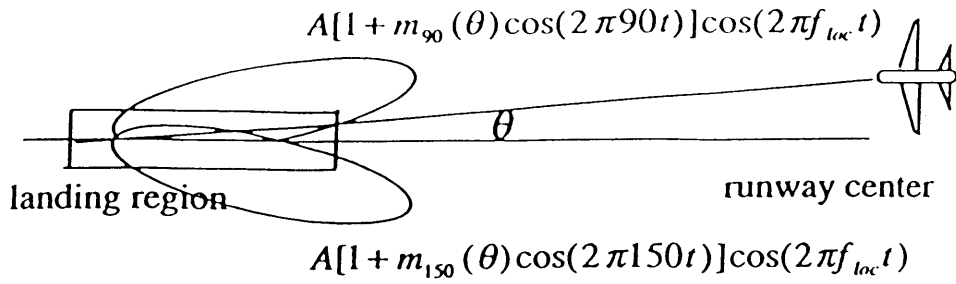
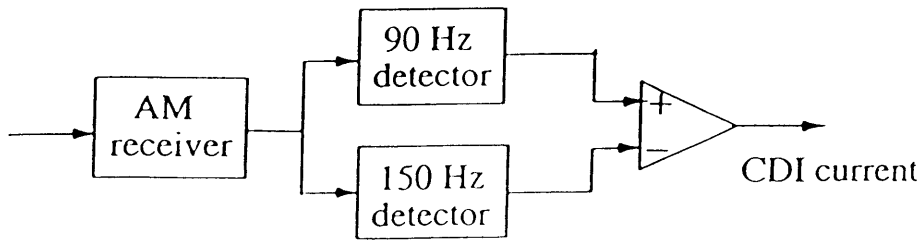


Fig1.1 Instrument Landing System [2]

Localizer beam pattern:



ILS localizer receiver:



Angular dependence of DDM:

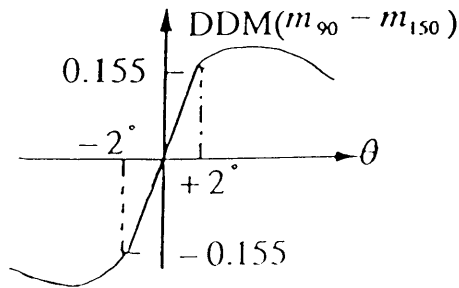


Fig1.2 ILS operating principle

1.3 TYPES OF RADIO INTERFERENCE TO ILS

Several physical mechanisms have been identified as possible causes of radio interference to ILS. They are divided into four classes by the International Telecommunication Union (ITU): A1, A2, B2 and B1. A1 is in-band interference. It refers to the condition when the input noise spectrum directly overlaps with localizer passband such that the amplitude of 90 Hz and 150 Hz subcarriers are changed. The band to cause A1 interference is very narrow: centered at the operating localizer frequency it spans the width of localizer passband (several hundreds Hz). Since no other radio communication than ILS localizer is allowed within 108.1 MHz to 111.95 MHz, the likely source of interference is the harmonics of transmitters at other bands.

A2 covers the general adjacent-band interference. It is generated by the noise with spectrum not exactly in but very close to localizer band such that part of it falls in the receiver passband. The noise cannot be completely got rid of before receiver baseband so the amplitudes of 90 Hz and 150 Hz subcarriers are changed accordingly. A2 happens only when both localizer channel and interference spectrum are very close to 108.1 MHz, for example, localizer channel 108.1 MHz and FM channel 107.9 MHz. When the radio frequency is far away from the desired receiver frequency but causes interference the mechanism is classified as B2. It occurs when the input noise power level is relatively high. Because of the high input power the mechanism responsible for B2 is probably receiver nonlinearity.

The type of interference dealt in this thesis is B1 – intermodulation interference. A1, A2 and B2 can be induced by one frequency, but B2 should be induced by two or more. Intermodulation is also the product of receiver nonlinearity. For a nonlinear system, the output includes not only those frequencies which are present in input excitation, but also numbers of harmonics which are the combinations of the input frequencies. Intermodulation interference to the receiver occurs when the receiver is driven into a nonlinear region of operation by high-powered signal such that the harmonics which lie within the receiver passband are generated and appeared at the

output. For the intermodulation to occur, at least two signals need to be present. And the harmonics are linear combinations of input frequencies. For example, if the input of a nonlinear device contains two frequencies f_1 and f_2 , then the second-order intermodulation components occur at $f_1 + f_2$ and $f_1 - f_2$, the third-order intermodulation components occur at $2f_1 + f_2$, $2f_1 - f_2$, $2f_2 + f_1$ and $2f_2 - f_1$, and so on. Even if all the interfering frequencies lie out of the receiver passband, their intermodulation components can fall right at the desired frequency. The proximity of FM broadcasting frequencies to ILS localizer band makes localizer receiver susceptible to FM-generated intermodulation interference.

1.4 OVERVIEW OF PROBLEM AND METHODOLOGY

The calculation of intermodulation products from multiple input frequencies has been known to be a tedious problem [11] [28]. In the past half century intensive study of intermodulation interference in communication and broadcasting technology have been conducted. Some of the most distinguishable cases of interest can be found in wireless communication circuits [6] [8] [13] [14] [22] and cable TV circuits [1] [4] [18] [22]. Most literature put emphasis on analyzing intermodulation effect of individual nonlinear device, for example, RF amplifiers and mixers. However, quantitative study of intermodulation on the whole system has been lacking. The latter is important for analyzing the interaction between RF systems and control systems, as in the case of ILS-driven aircraft automatic landing system. Only when we construct the model of whole system on the basis of available empirical data can we achieve this goal.

Out of this concern, the aviation community has studied ILS interference problem through a series of bench experiments on different kinds of operational receivers. These experiments consist of measuring the “threshold” of interfering power as a function of frequency under A1, A2/B2 and B1 conditions. Regression formula derived from the performance of typical receivers were derived. These empirical formula is important for radio environment evaluation since they specify the cut-off level at which interfering power is considered intolerable.

However, the regression curves specify the threshold conditions only. They do not provide the information of ILS response to the cases under or above the threshold conditions. This information is important for the overall simulation of aircraft landing process. Therefore a receiver simulation model is necessary. Since it is impossible to run the detailed simulation for all kinds of ILS receivers on the market, we develop a “generic” model based on the regression formula. The methodology is described as follows: (1) Based on real operations of ILS receivers and certain acceptable assumptions, a simplified mathematical model is derived. This model is characterized by a set of parameters. (2) The parameter values are inverted from a set of regression

curves. In this thesis two-frequency B1 curves are chosen as the objective to be fitted.

(3) Apply the model to other conditions and compare the simulation results with new regression curves to verify the consistency of the generic receiver model.

The following chapters are arranged as follows: Chapter two is the detailed description of mathematical model. It includes frequency selection stage which converts RF into IF signal and baseband stage which extracts course deviation current from IF signal. Chapter three is the synthesis of receiver model with respect to empirical results. It contains the experimental procedures for ILS B1 test, regression formula for experimental results, inversion procedures for retrieving values of parameters, the values of receiver parameters inverted from regression formula of two-frequency intermodulation, and simulated threshold curves. Chapter four extends current model to different interference conditions. It includes the extrapolation of future-standard ILS receivers, simulation on pure-carrier intermodulation interference and CDI calculation under non-threshold interference conditions.

Chapter 2

Generic Model for ILS Receiver

2.1 LOCALIZER RECEIVER ARCHITECTURE

The configuration of localizer receiver is in Figure 2.1. There are two principal stages in the receiver. The first stage, or frequency selection stage, recovers baseband signal from its amplitude-modulated form. It functions like a regular AM receiver, converting RF input into baseband output. At the very front an RF section filters and amplifies the input. Its output is fed into a mixer which multiplies the incoming RF signal by a local oscillator carrier to down-convert the operating frequency to IF. The IF signal is filtered and amplified in IF section. After IF an envelope detector is followed to detect the amplitude of IF output. Baseband signal is retrieved at the output of envelope detector. In addition to RF, mixer and IF, Automatic Gain Control (AGC) which confines the output power level of frequency selection stage within a narrow range is also incorporated.

Generic Model for ILS Receivers

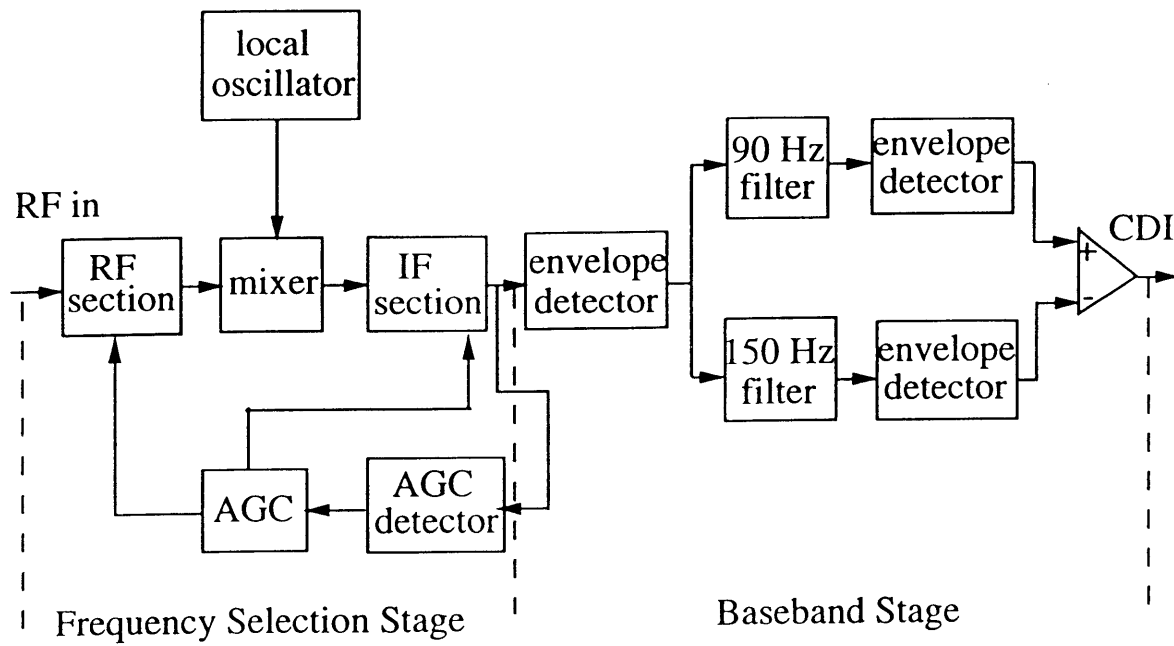


Fig2.1 ILS receiver configuration

The second stage converts processed IF signal into Course Deviation Indicator (CDI) current. We shall call it baseband stage. Baseband signal is splitted into two paths: the first one contains a 90 Hz-centered bandpass filter and an envelope detector, the second one contains an 150 HZ-centered bandpass filter and an envelope detector. The output of the two paths are fed into a differential amplifier to get the course deviation current. Among all the sections IF envelope detector is the interface between the frequency selection stage and the baseband stage. In the following paragraphs IF envelope detector is attributed as a part of baseband stage.

A generic receiver model is built by linking all the models of function blocks in Figure 2.1 and cascading them together. The following sections will discuss the construction of frequency-selection-stage model and baseband-stage model in more detail. The modeling of a single nonlinear device is necessary before starting a macroscopic consideration.

2.2 MODELING OF A NONLINEAR DEVICE

Intermodulation interference is the result of receiver nonlinearity. For modeling purpose, we consider a nonlinear system S with one input $x(t)$ and one output $y(t)$. Similar to the way a linear system is represented by an impulse response $h(t)$, a nonlinear system will be represented by a series of impulse responses $h_1(t)$, $h_2(t_1, t_2)$, $h_3(t_1, t_2, t_3)$, such that

$$y(t) = \sum_{i=1}^{\infty} \int_{-\infty}^{\infty} \cdots \int_{-\infty}^{\infty} d\tau_1 \cdots d\tau_i h_i(\tau_1, \dots, \tau_i) x(t - \tau_1) \cdots x(t - \tau_i) \quad (2.2.1)$$

The form of (2.2.1) is called the Volterra-series representation [27] [29]. This representation takes into account not only high-order terms due to nonlinearity but also the temporal variation. In general $y(t)$ cannot be expanded into a power series of $x(t)$ but is an integral-transform type series with which transfer functions $h_1(t)$, $h_2(t_1, t_2)$, are involved.

Rather than sticking to this rigorous but complicated proposition, the thesis assumed that output $y(t)$ is a functional of input $x(t)$.

$$y(t) = F(x(t)) \quad (2.2.2)$$

This assumption is correct if the operating amplitude and frequency are within reasonable regions. For example, to the first-order approximation the capacitive effect of a PN junction could be ignored and diode current (output) $I_d(t)$ is related to diode voltage $V_d(t)$ by the formula $I_d(t) = I_0(\exp(V_d(t)/V_T) - 1)$. The source of ILS receiver nonlinearity is mainly amplifier. It is well known that temporal variation is secondary in nonlinear amplifiers like FET or BJT. Modeling i/o relationship as a functional is a valid approximation. If y is a function of x then it could be expanded into a power series of x :

$$y = \sum_{i=1}^{\infty} K_i x^i \quad (2.2.3)$$

How many terms should we keep in order to cover the dominant nonlinear effect depends on the function itself and input amplitude. For a nonlinear amplifier, the input/output relationship usually resembles a curve like the one in Figure 2.2.

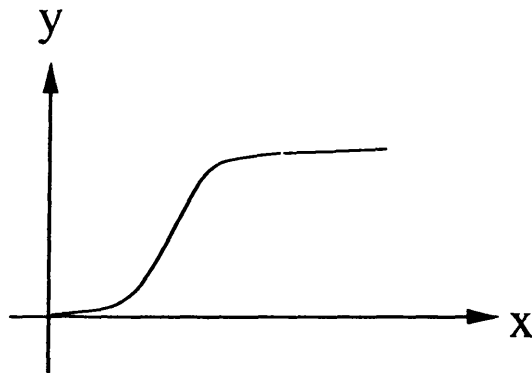


Fig2.2 Typical nonlinear input/output relationship

The operational region, could be approximated by a low-order polynomial. If input amplitude is not high enough to drive output into saturation, then it is valid to model a nonlinear device as a low-order polynomial:

$$y \approx \sum_{i=1}^N K_i x^i \quad (2.2.4)$$

This thesis concentrates on the third-order approximation. For the case of FM (88.1 to 107.9 MHz) intermodulation interference on ILS localizer (108.1 to 111.95 MHz) the second-order term $K_2 x^2$ generates harmonics far beyond localizer frequency (either $f_{loc} - f_{FM}$ or $f_{loc} + f_{FM}$), so it is sufficient to keep only two terms: linear and the third-order:

$$y \approx K_1 x + K_3 x^3 \quad (2.2.5)$$

Intermodulation interference generated by a single nonlinear device could be calculated by using this model. Consider the case where N interfering components $A_i \cos(2\pi f_i t + \phi_i)$ along with a desired component $A_0 \cos(2\pi f_0 t)$ enter the device:

$$x(t) = A_0 \cos(2\pi f_0 t) + \sum_{i=1}^N A_i \cos(2\pi f_i t + \phi_i) \quad (2.2.6)$$

The output $y(t) = K_1x(t) + K_3x(t)^3$ contains linear part $x(t)$ (see (2.2.6)), and nonlinear part $x(t)^3$:

$$\begin{aligned}
x(t)^3 &= \sum_{i=0}^N \frac{A_i^3}{4} [\cos(3(2\pi f_i t + \phi_i)) + 3 \cos(2\pi f_i t + \phi_i)] \\
&+ \sum_{0 \leq i < j \leq N} 3 \left[\frac{A_i^2 A_j}{2} \cos(2\pi f_j t + \phi_j) + \frac{A_j^2 A_i}{2} \cos(2\pi f_i t + \phi_i) \right. \\
&\quad + \frac{A_i^2 A_j}{4} \cos(2\pi(2f_i + f_j)t + 2\phi_i + \phi_j) \\
&\quad + \frac{A_i^2 A_j}{4} \cos(2\pi(2f_i - f_j)t + 2\phi_i - \phi_j) \\
&\quad + \frac{A_j^2 A_i}{4} \cos(2\pi(2f_j + f_i)t + 2\phi_j + \phi_i) \\
&\quad \left. + \frac{A_j^2 A_i}{4} \cos(2\pi(2f_j - f_i)t + 2\phi_j - \phi_i) \right] \\
&+ \sum_{0 \leq i < j < k \leq N} \frac{3}{2} A_i A_j A_k [\cos(2\pi(f_i + f_j + f_k)t + \phi_i + \phi_j + \phi_k) \\
&\quad + \cos(2\pi(-f_i + f_j + f_k)t - \phi_i + \phi_j + \phi_k) \\
&\quad + \cos(2\pi(f_i - f_j + f_k)t + \phi_i - \phi_j + \phi_k) \\
&\quad + \cos(2\pi(f_i + f_j - f_k)t + \phi_i + \phi_j - \phi_k)] \tag{2.2.7}
\end{aligned}$$

where $i = 0$ represents desired signal.

The output sinusoidal components with frequency f_0 are:

$$(a) \quad K_1 A_0 \cos(2\pi f_0 t)$$

$$(b) \quad \frac{3}{4} K_3 A_0^3 \cos(2\pi f_0 t)$$

$$(c) \quad \sum_{i=1}^N \frac{3}{2} K_3 A_0 A_i^2 \cos(2\pi f_0 t)$$

$$(d) \quad \sum_{2f_i - f_j = f_0} \frac{3}{4} A_i^2 A_j \cos(2\pi(2f_i - f_j)t + 2\phi_i - \phi_j)$$

$$(e) \quad \sum_{f_i + f_j - f_k = f_0} \frac{3}{2} A_i A_j A_k \cos(2\pi(f_i + f_j - f_k)t + \phi_i + \phi_j - \phi_k)$$

(a) is the linear term. (b) is generated by third-order intermodulation of localizer frequency with itself, $f_0 - f_0 + f_0$. It is named ‘self-modulation’ component [23]. (c) is generated by third-order intermodulation of localizer frequency with one interfering frequency, $f_i - f_i + f_0$. It is named ‘cross-modulation’ components [22]. (d) and (e) are generated by third-order intermodulation of two and three interfering frequencies. (b) and (c) have exactly the same spectra as localizer signal (a) since no $\phi_i(t)$ appears in the phases. They essentially modifies the amplitude of localizer signal but eventually would not effect the output CDI value. So (b) and (c) can be seen as parts of signal. Combination of (d) and (e) is third-order intermodulation interference generated by device nonlinearity. To summarize, the signal part at output is

$$[K_1 A_0 + \frac{3}{4} K_3 A_0^3 + \sum_{i=1}^N \frac{3}{2} K_3 A_0 A_i^2] \cos(2\pi f_0 t)$$

And the interference part is

$$\sum_{2f_i - f_j = f_0} \frac{3}{4} K_3 A_i^2 A_j \cos(2\pi f_0 t + 2\phi_i - \phi_j) +$$

$$\sum_{f_i + f_j - f_k = f_0} \frac{3}{2} K_3 A_i A_j A_k \cos(2\pi f_0 t + \phi_i + \phi_j - \phi_k)$$

Let the summation of these two parts equal to $y(t)$. Its total amplitude depends on phases ϕ_1, ϕ_2, \dots . In the case of ILS localizer, the most serious source of intermodulation interference is FM broadcasting. The phases of FM carriers are the messages to be transmitted, therefore they are functions of time. In general they are stochastic processes and uncorrelated with one another. The ensemble average power of $y(t)$ is the summation of coherent (signal) power and incoherent (interference) power:

$$\begin{aligned}
 2 \langle y(t)^2 \rangle = & [K_1 A_0 + \frac{3}{4} K_3 A_0^3 + \sum_{i=1}^N \frac{3}{2} K_3 A_0 A_i^2] \\
 & + \sum_{2f_i - f_j = f_0} \frac{9}{16} K_3^2 A_i^4 A_j^2 + \sum_{f_i + f_j - f_k = f_0} \frac{9}{4} K_3^2 A_i^2 A_j^2 A_k^2 \quad (2.2.8)
 \end{aligned}$$

Taking the square root of average power to be the effective amplitude, the f_0 component at the output becomes

$$y(t) \approx \sqrt{\langle y(t)^2 \rangle} \cos(2\pi f_0 t + \phi) \quad (2.2.9)$$

Equation (2.2.8) and (2.2.9) apply to other frequencies as well. They provide the formulation to calculate a nonlinear device's output.

2.3 MODELING OF FREQUENCY SELECTION STAGE

In a receiver the RF signal should be processed and converted into baseband signal. This is done by frequency selection stage. As indicated in Figure 2.1, the frequency selection stage consists of RF, mixer, and IF sections, like a typical AM receiver. A realistic AM receiver may have more than one IF section. In our simplified model only one IF section is presented. This should not, however, affect the simulation results significantly.

In the frequency selection stage model we also only need to treat either localizer signal or undesired FM interference at a specific broadcasting frequency like a pure carrier, and leave those detailed phase terms to the baseband signal processing stage. For the localizer component, we take the root mean square of the slowly-varying envelope as effective amplitude:

$$A_{loc}^{in} [1 + m_{90} \cos(2\pi \cdot 90t) + m_{150} \cos(2\pi \cdot 150t)] \approx A_{loc}^{in} \sqrt{[1 + 0.5m_{90}^2 + 0.5m_{150}^2]} \quad (2.3.1)$$

The value of modulation index m_{90} and m_{150} is between 0.2775 and 0.1125 in the operation range of localizer. Under most cases it is valid to assume $m_{90} \approx m_{150} \approx 0.2$. Therefore the effective amplitude can be further approximated:

$$A_{loc}^{in} [1 + m_{90} \cos(2\pi \cdot 90t) + m_{150} \cos(2\pi \cdot 150t)] \approx A_{loc}^{in} \sqrt{1.04} \quad (2.3.2)$$

Instead of having a temporally varying amplitude, the FM interference contains a temporally varying phase. To treat it as a pure carrier, we assume the slowly varying phase function is approximately a constant:

$$A_{FM}^{in} \cos(2\pi f_{FM}t + \phi(t)) \approx A_{FM}^{in} \cos(2\pi f_{FM}t + \phi) \quad (2.3.3)$$

The pure-carrier approximation is valid since either the localizer signal bandwidth (no more than several KHz) or the FM bandwidth (64 KHz for standard test condition, see [20]) is much narrower than RF (88 to 112 MHz), RF bandwidth (several MHz) and IF center frequency (5 to 30 MHz).

2.3.1 RF Section

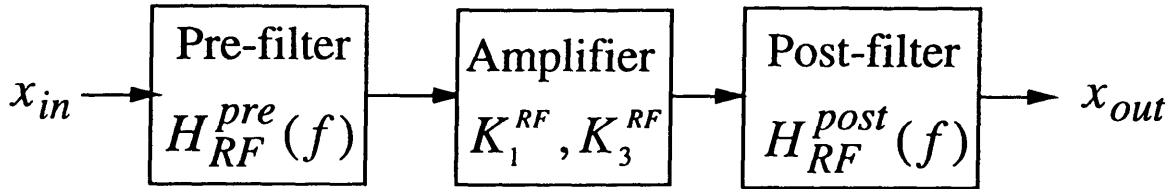


Fig2.3 RF-section block diagram

Figure 2.3 is a RF-section block diagram. It contains an RF pre-filter, an amplifier and a post-filter. A pre-filter is often a tuned LC circuit or other equivalent passive bandpass filter. It can be characterized by a frequency response function $H_{RF}^{pre}(f) = |H_{RF}^{pre}(f)| \exp(i\phi_{RF}^{pre}(f))$. For an input $x(t) = \sum_{i=1}^N A_i \cos(2\pi f_i t + \phi_i)$, the output of pre-filter is $y(t) = \sum_{i=1}^N |H_{RF}^{pre}(f_i)| A_i \cos(2\pi f_i t + \phi_i + \phi_{RF}^{pre}(f_i))$. Typically $|H_{RF}^{pre}(f)|$ peaks around the center frequency f_c and drops monotonically on both sides. The center frequency f_c is usually tunable with localizer frequency f_{loc} . The filter transfer function is usually normalized such that the peak value is unity. Here we adopt the same convention to split RF pre-filter characteristics into two parameters: normalized filter response and front-end gain:

$$H_{RFold}^{pre}(f) = A_{RF}^{pre} \cdot H_{RF}^{pre}(f) \quad (2.3.4)$$

where $|H_{RF}^{pre}(f_c)| = 1$.

The RF post-filter is modeled exactly the same way as pre-filter except with a different frequency response $H_{RF}^{post}(f)$ and normalization constant A_{RF}^{post} .

The RF amplifier is often a transistor device such as field effect transistor (FET). The effect of temporal variation in this kind of device is considered secondary within the operating frequency range. However its nonlinear effect cannot be ignored. The model described in Section 2.2 could apply here. From experiments it is observed that nonlinearity of RF amplifier K_3/K_1 varies with different input power levels [7]. In this thesis, third-order nonlinearity is specified at few discrete input power levels.

Given $H_{RF}^{pre}(f)$, A_{RF}^{pre} , K_3 , K_1 , $H_{RF}^{post}(f)$, A_{RF}^{post} and input amplitude for each frequency component, the amplitude of each frequency at RF output could be evaluated. Ideally a pre-filter is very selective so that all interference other than localizer frequency is suppressed. But it is difficult to implement such a filter. Separation between localizer and FM is less than 200 KHz, a bandwidth RF filters could hardly achieve. Thus significant amount of energy in the FM signal can pass the filter and cause intermodulation interference. The interference amplitude is a function of pre-filter response at input FM frequencies $H_{RF}^{pre}(f_1)$, $H_{RF}^{pre}(f_2)$, If RF pre-filter and post-filter cannot suppress interference well, then nonlinearity after RF section has to be considered. In this case mixer would produce non-negligible intermodulation interference.

2.3.2 Mixer

Mixer is also a nonlinear device. Unlike an amplifier, a mixer has two input: one is from RF section and the other is from local oscillator. Ideally the output of a mixer is the product of two inputs. Without interference, the RF-section output is pure localizer signal $x(t) = A0_{loc}^{RF} \cos(2\pi f_{loc}t)$. The local oscillator output is a pure sinusoidal wave $x_{osc}(t) = A_{osc} \cos(2\pi f_{osc}t + \phi_{osc})$, where the frequency difference between both is IF, $|f_{osc} - f_{loc}| = f_{IF}$. f_{osc} could be larger or smaller than f_{loc} . In the model we assume a superheterodyne receiver, i.e. $f_{osc} - f_{loc} = f_{IF}$. Thus the ideal mixer output $y(t)$ is

$$y(t) = x(t) \cdot x_{osc}(t) = A0_{loc}^{RF} A_{osc}/2 [\cos(2\pi(f_{osc} + f_{loc})t + \phi_{osc}) + \cos(2\pi(f_{osc} - f_{loc})t + \phi_{osc})] \quad (2.3.5)$$

The first term, which is far above the IF band, can be removed by the IF filter.

A real mixer contains more terms than (2.3.5). We consider the following approximation model represented by the fourth-order Taylor series expansion over two variables: Generally a mixer is a nonlinear 'three-port'. The output y is a function of x and x_{osc} . It can be expanded into a Taylor series

$$\begin{aligned} y = f(x, x_{osc}) &= f(x^o, x_{osc}^o) + \left(\frac{\partial f}{\partial x}\right)_o x + \left(\frac{\partial f}{\partial x_{osc}}\right)_o x_{osc} \\ &+ \left(\frac{\partial^2 f}{\partial x^2}\right)_o x^2 + 2\left(\frac{\partial^2 f}{\partial x \partial x_{osc}}\right)_o x x_{osc} + \left(\frac{\partial^2 f}{\partial x_{osc}^2}\right)_o x_{osc}^2 \\ &+ \left(\frac{\partial^3 f}{\partial x^3}\right)_o x^3 + 3\left(\frac{\partial^3 f}{\partial x^2 \partial x_{osc}}\right)_o x^2 x_{osc} + 3\left(\frac{\partial^3 f}{\partial x \partial x_{osc}^2}\right)_o x x_{osc}^2 + \left(\frac{\partial^3 f}{\partial x_{osc}^3}\right)_o x_{osc}^3 \\ &+ \left(\frac{\partial^4 f}{\partial x^4}\right)_o x^4 + 4\left(\frac{\partial^4 f}{\partial x^3 \partial x_{osc}}\right)_o x^3 x_{osc} + 6\left(\frac{\partial^4 f}{\partial x^2 \partial x_{osc}^2}\right)_o x^2 x_{osc}^2 \end{aligned}$$

$$+4 \left(\frac{\partial^4 f}{\partial x \partial x_{osc}^3} \right)_o x x_{osc}^3 + \left(\frac{\partial^4 f}{\partial x_{osc}^4} \right)_o x_{osc}^4 + H.O.T. \quad (2.3.6)$$

where O represents operating point, e.g. $\left(\frac{\partial f}{\partial x} \right)_o$ means the value of function $\left(\frac{\partial f}{\partial x} \right)$ at the operating point $(x, x_{osc}) = (x^o, x_{osc}^o)$. *H.O.T.* refers to high-order terms.

It is obvious that in (2.3.6) the odd-order terms do not lie in the IF passband provided input frequencies are not far from RF. Unlike a nonlinear amplifier, the relevant intermodulation components of a mixer are second-order, fourth-order, ... and so on. $x x_{osc}$ provides desired localizer signal, x^2 and x_{osc}^2 generate baseband frequencies and fourth order plays the role of amplifier's third order. For example, if there are two interfering frequencies f_1 f_2 satisfying $2f_1 - f_2 = f_{loc}$, then $x^3 x_{osc}$ would produce intermodulation term with frequency $f_{osc} - f_1 - f_1 + f_2$ which is exactly equal to f_{IF} ($f_{osc} - f_{loc}$).

Eight terms in (2.3.6) should be kept (second and fourth order) to include both linear and third-order intermodulation effects. This means generally a mixer is characterized by eight coefficients, which makes the model more complicated. We shall consider a simpler but realistic situation, i.e. the balanced mixer. The balanced mixer uses two symmetric nonlinear devices to eliminate the first-order components. Its configuration is in Figure 2.4.

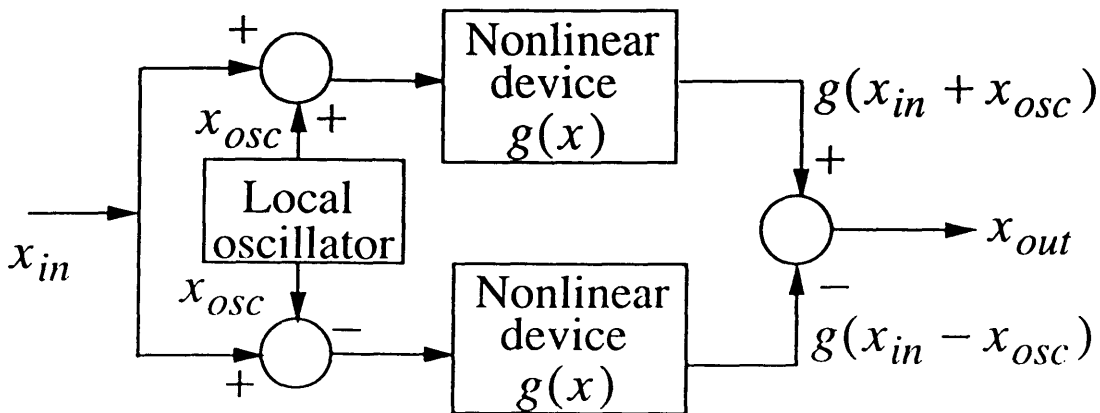


Fig2.4 Block diagram of a balanced mixer

The output of a balanced mixer $y(t)$ is a nonlinear function of x and x_{osc} with form:

$$y = g(x + x_{osc}) - g(x - x_{osc}) = g^{(1)}(o) \cdot 2x_{osc} + g^{(2)}(o) \cdot 2xx_{osc} + 1/3g^{(3)}(o) \cdot (3x^2x_{osc} + x_{osc}^3) + 1/3g^{(4)}(o) \cdot (x^3x_{osc} + x_{osc}^3x) + H.O.T. \quad (2.3.7)$$

Among the lower-order terms in (2.3.7) the ones capable of generating IF are $g^{(2)}(o) \cdot 2xx_{osc}$ and $1/3g^{(4)}(o) \cdot (x^3x_{osc} + x_{osc}^3x)$. Let $2g^{(2)}(o) = K_2$, $1/3g^{(4)}(o) = K_4$, $x = \sum_{n=1}^N A_n \cos(2\pi f_n t + \phi_n)$ and $x_{osc} = A_{osc} \cos(2\pi f_{osc} t + \phi_{osc})$. Substitute into (2.3.7) and get rid of out-of-IF-band components, the resultant y would be

$$y = (1/2K_2A_{osc} + 3/8K_4A_{osc}^3) \sum_{n=1}^N A_n \cos(2\pi(f_{osc} - f_n)t + \phi_{osc} - \phi_n) + 1/2K_4A_{osc} \sum_{m=1}^M B_m \cos(2\pi(f_{osc} - f_m)t + \phi_{osc} - \phi_m) \quad (2.3.8)$$

where $\sum_{m=1}^M B_m \cos(2\pi f_m t + \phi_m) = \sum_{n=1}^N A_n \cos(2\pi f_n t + \phi_n)^3$.

Therefore the operation of balanced mixer resembles that of a nonlinear amplifier with linear coefficient $1/2K_2A_{osc} + 3/8K_4A_{osc}^3$ and third-order nonlinear coefficient $1/2K_4A_{osc}$, except that every sinusoid contains a phase difference ϕ_{osc} . Only two coefficients are required to characterize a balanced mixer.

2.3.3 IF Section

Generally IF section is similar to RF section, but they differ from each other in several aspects. The IF filter is much more selective than the RF filter. In the case of ILS localizer the 3-dB bandwidth is usually no more than 100 KHz, and at least 60 to 80 dB attenuation would be reached for the FM interference. The IF amplifier can also achieve higher gain than is possible for RF amplifier. A common IF circuit consists of a highly selective crystal filter followed by a series of cascading amplifiers. The crystal filter corresponds to IF pre-filter. Typically IF filters used in localizer receivers are implemented as Chebyshev filters having order 6, 8 or 10 [26]. For the worst-case consideration, sixth-order Chebyshev filter is used in receiver model. It has the magnitude response:

$$|H_{IF}^{pre}(f)| = \frac{1}{\sqrt{1 + 1.512T_1^2(f)}} \quad (2.3.9)$$

where $T_1(f) = 4T_0^3(f) - 3T_0(f)$, $T_0(f) = \frac{(f_{IF}^2 - f^2)}{BW \cdot f}$

The frequency response of sixth-order Chebyshev filter is demonstrated in Figure 2.5.

The amplifier set is not only a nonlinear device but also contains RC circuits that serve as filters. It corresponds to IF amplifier and IF post-filter. Notice that IF amplifier may perform a better linearity either because more linear device could be used (e.g. BJT) or more delicate design could be applied to reduce nonlinearity (e.g. log amplifier) under lower frequency range. Because IF pre-filter is highly selective, intermodulation at the IF amplifier is negligible unless incoming FM interference is extremely large. In our receiver model IF section is characterized by a sixth-order Chebyshev pre-filter H_{IF}^{pre} , a 'good' amplifier with large linear gain K_1^{IF} and negligible nonlinear coefficient K_3^{IF} , and a flat post-filter H_{IF}^{post} . Figure 2.6 is IF-section block diagram.

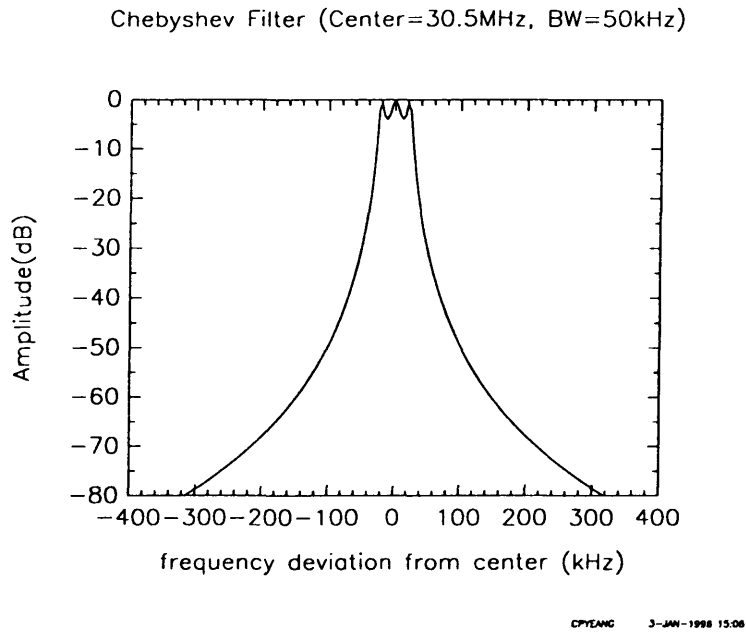


Fig2.5 Sixth-order Chebyshev filter

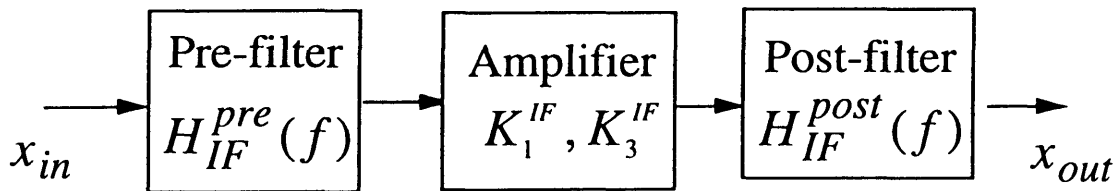


Fig2.6 IF-section block diagram

2.3.4 Automatic Gain Control

Automatic Gain Control (AGC) is the mechanism that keeps output voltage approximately at a constant level. AGC is a simple feedback control system. Its structure is indicated in Figure 2.7a. An AGC detector at the IF output is responsible for the detection of output voltage level. Sometimes it is just the IF envelope detector. When the input level increases too much such that output level exceeds the allowable range, the detected level from AGC detector drives AGC control circuit to decrease the RF as well as IF amplifier gain. Therefore output voltage level comes back within range. The reverse operation is carried out when input level is too low. For an ILS localizer receiver AGC is necessary to implement in frequency selection stage in order to fix the voltage level at the output of IF envelope detector (see Figure 2.1).

In practical term, we need to consider several points to implement the AGC simulation model. First, the term “voltage level” is ambiguous. What is the exact quantity to trigger AGC operation? The purpose of AGC is to confine the envelope level of IF output so that the output of AM detector (i.e. the input of baseband stage) is roughly a constant. With respect to this consideration the time average of envelope-detected output is a good measurable. But to obtain this quantity one would need the knowledge of individual phase terms. To avoid the complication in involving the phase we use another quantity as the AGC input: the square root of the sum of the amplitudes at all frequency components. For an IF output $\sum_i A_i \cos(2\pi f_i t + \phi_i)$, the average amplitude level $\sqrt{\sum_i \frac{1}{2} A_i^2}$ should lie within the designated range, or else AGC is triggered to pull it back.

The exact mathematical relationship between IF average amplitude level and linear/nonlinear coefficients of RF/IF amplifier is determined by circuit analysis, and varies with different kinds of receivers. For a generic receiver model the following iterative algorithm is a reasonable approximation: if the output level is beyond upper (or lower) limit of the designated range, then K_1^{RF} , K_3^{RF} , K_1^{IF} , and K_3^{IF} are decreased (or increased) in small steps. The same input is applied and the same process is repeated again until the output level falls into the specified range. This mechanism is indicated in Figure 2.7b. The underlying assumption of this model is that RF/IF nonlinearity K_3/K_1 keeps exactly the same no matter how large the automatic gain control signal is fed into the amplifier. However it is not always true. Take an FET amplifier as an example. The gain of an FET amplifier is controlled by gate voltage. When different gate voltage values are applied, the amplifier has different i/o curves. These curves could have different nonlinearity K_3/K_1 near the operating point. This problem becomes worse when input level is so large that amplifier is saturated, which means the polynomial model is no more appropriate for the amplifier. If input localizer and interference power is small enough such that the amplifiers are still 'weakly nonlinear', then the above assumption is valid.

Therefore AGC could be simulated in the following procedures.

- (1) Pick up initial values for K_1^{RF} , K_3^{RF} , K_1^{IF} , K_3^{IF} .
- (2) Run the frequency-selection stage simulation
- (3) If the summation of every sinusoidal component's mean power at IF output is above/below the prescribed range, then decrease/increase K_1^{RF} , K_3^{RF} , K_1^{IF} , K_3^{IF} by the same ratio. Go to (2).

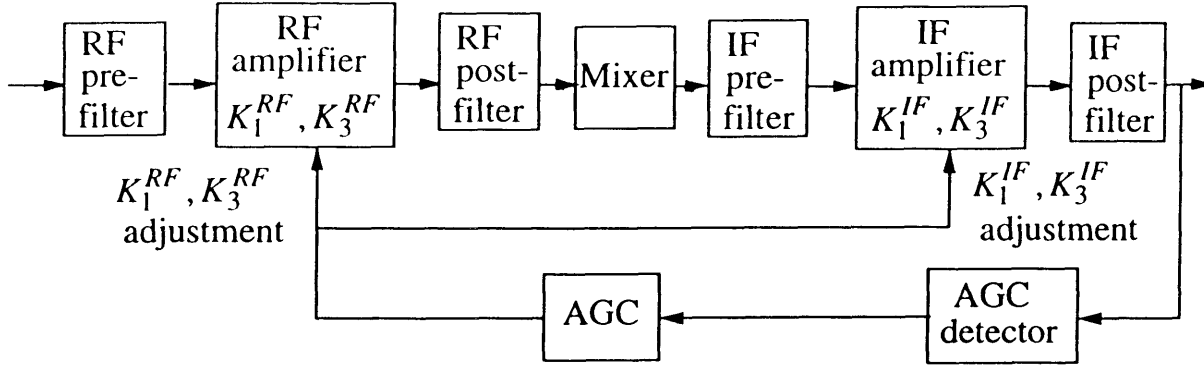
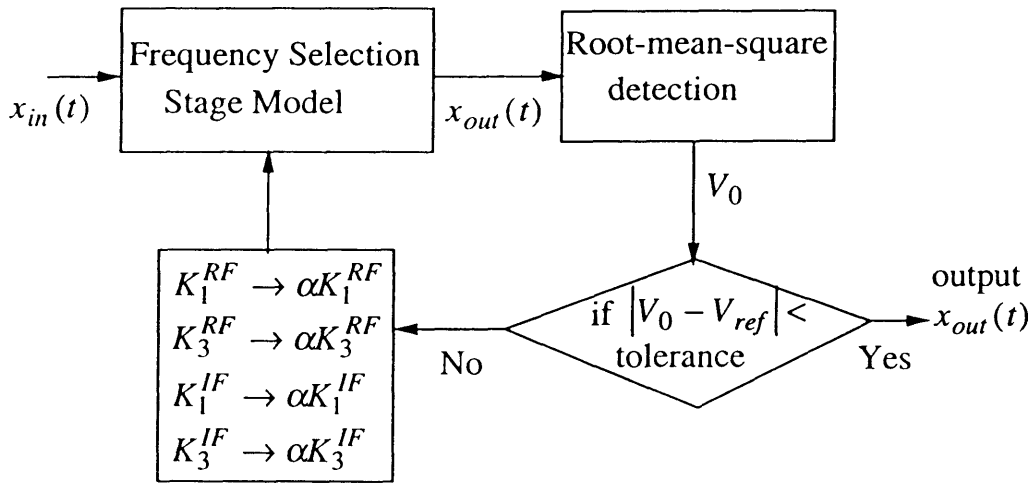


Fig2.7a Configuration of AGC



Root-mean-square detection:

$$x_{out}(t) = \sum_{m=1}^N A_m \cos(2\pi f_m t + \phi_m)$$

$$V_0 = \sum_{m=1}^N A_m^2$$

Fig2.7b Procedures for AGC simulation

2.4 MODELING OF BASEBAND STAGE

The localizer signal at IF output

$$A_{loc}^{IF}[1 + m_{90} \cos(2\pi \cdot 90t) + m_{150} \cos(2\pi \cdot 150t)] \cos(2\pi f_{IF}t)$$

is converted into CDI output $A_{loc}^{base}(m_{90} - m_{150})$ via the baseband stage. As indicated in Figure 2.1, the IF signal is processed by an envelope detector first. The amplitudes of 90 Hz and 150 Hz components are retrieved by a 90 Hz and a 150 Hz detector and are passed through a comparator to get the CDI output. Unlike frequency selection stage, the baseband stage model is a statistical model because the interference signal is random in nature. We should apply the Monte Carlo technique. The objective of this section is to construct a simple relation of CDI with IF interfering power, given modulation depth m_{90} and m_{150} .

2.4.1 Conversion of Frequency Selection Output Into Baseband Input

There is an essential distinction between the frequency selection stage model and baseband stage model. Frequency selection stage model treats either localizer signal or undesired FM interference at a specific broadcasting channel as a pure carrier. Its task is to evaluate the frequency and amplitude of each carrier at IF output. So the IF output x_{out}^{IF} calculated by model can be represented as follows:

$$x_{out}^{IF} = A0_{loc}^{IF} \cos(2\pi f_{IF}t) + A_{intf}^{IF} \cos(2\pi f_{IF}t + \phi_{intf}^{IF}) + \sum_{i=1}^N A_i \cos(2\pi f_i t + \phi_i) \quad (2.4.1)$$

where $A_{intf}^{IF} \cos(2\pi f_{IF}t)$ is the intermodulation interference with frequency exactly at localizer IF.

On the other hand, baseband stage should take the temporal variation of localizer amplitude and FM phase, which were hidden in frequency selection stage model, into account since its objective is to detect out the very low frequency components. So the detector input x_{in}^{det} should be

$$x_{in}^{det} = A_{loc}^{IF} [1 + m_{90} \cos(2\pi \cdot 90t) + m_{150} \cos(2\pi \cdot 150t)] \cos(2\pi f_{IF}t) + A_{intf}^{IF} \cos(2\pi f_{IF}t + \phi_{intf}^{IF}(t)) + \sum_{m=1}^N A_m \cos(2\pi f_m t + \phi_m(t)) \quad (2.4.2)$$

Frequency selection stage model only provides each component's amplitude value (A_{loc}^{IF} , A_{intf}^{IF} , or A_i) and frequency value (f_{IF} or f_i). It doesn't provide the information of modulation indices m_{90} and m_{150} and phase functions $\phi_{intf}^{IF}(t)$ and $\phi_i(t)$. Modulation indices are inherent in localizer input. They are set at the beginning. Phase functions are important parts of the FM signal. The baseband stage model should include their effect. The phase function of an FM input channel is time integration of audio message. It may also involve more signal processing like stereo and pre-emphasis in frequency domain in order to improve the performance [20]. In the model we convert the effect of phase functions on baseband stage to the effect of spectra. Each RF input component is not treated as a carrier with varying phase in time domain, but a collection of multiple frequencies with a specific spectrum, so does the IF output components in (2.4.2). Take for example the third-order intermodulation product $f_1 + f_2 - f_3$. Suppose at IF output the amplitude of this component (as evaluated by frequency selection stage model) is A , then its spectrum is approximately the convolution of three FM channels f_1 , f_2 and f_3 , with center frequency $|f_1 + f_2 - f_3 - f_{osc}|$, and total power $0.5A^2$. (Strictly speaking, the resultant spectrum is derived from (1) the convolution of f_1 , f_2 and f_3 channels after RF pre-filter, and (2) the convolution of IF impulse response with (1). The spectra after RF filter are slightly different from those of FM input spectra. And the product's spectrum after IF is slightly different from that at RF section.) Mathematically, the conversion of phase-function effect in (2.4.2) into continuous spectrum is the implementation of Fourier transform:

$$A_i \cos(2\pi f_m t + \phi_m(t)) = \int_{-\infty}^{+\infty} df H_m(f) \exp(i \cdot 2\pi f t) \quad (2.4.3)$$

Under intermodulation condition, the dominant interference term is the one with carrier frequency exactly the same as localizer signal, i.e. $A_{intf}^{IF} \cos(2\pi f_{IF} t + \phi_{intf}^{IF}(t))$ in (2.4.2). The other interfering components are suppressed to a large extent by IF filter. Even though some are passed, they usually fail to penetrate the extremely sharp baseband filters. Therefore this kind of noise could desensitize CDI output value via automatic gain control, but has no direct contribution to ‘in-band’ interference. The only spectrum we need to model at IF output is that of $A_{intf}^{IF} \cos(2\pi f_{IF} t + \phi_{intf}^{IF}(t))$. Notice that the FM noise can not be seen as deterministic. It is a stochastic process, so is its spectrum.

2.4.2 The Construction of Baseband Stage Model

Several observations are essential for the construction of an accurate and simple baseband stage model.

(1) It has been shown in Section 2.4.1 that in baseband stage input (2.4.2) only three variables are relevant: localizer amplitude A_{loc}^{IF} , IM interfering amplitude A_{intf}^{IF} and spectrum of IM interference. Given these three variables the CDI value could be calculated.

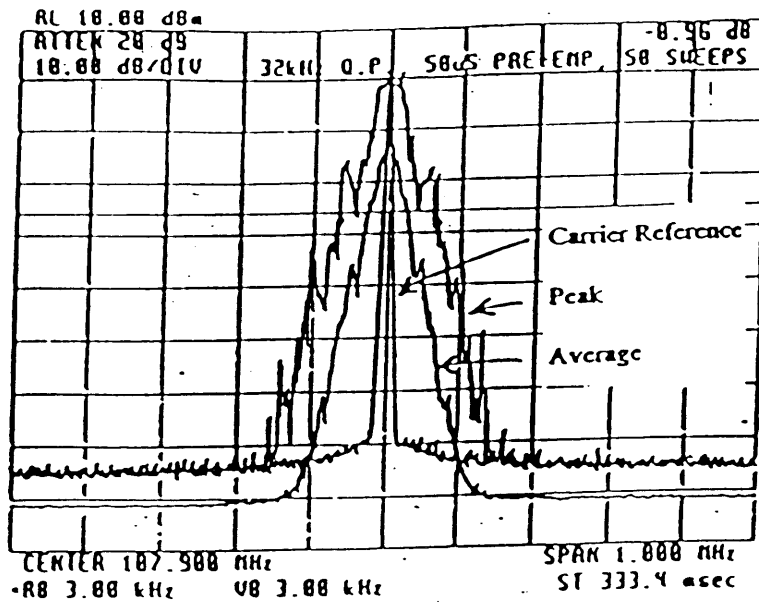


Fig2.8a FM power spectrum [20]. The 20-dB bandwidth is 64 KHz.

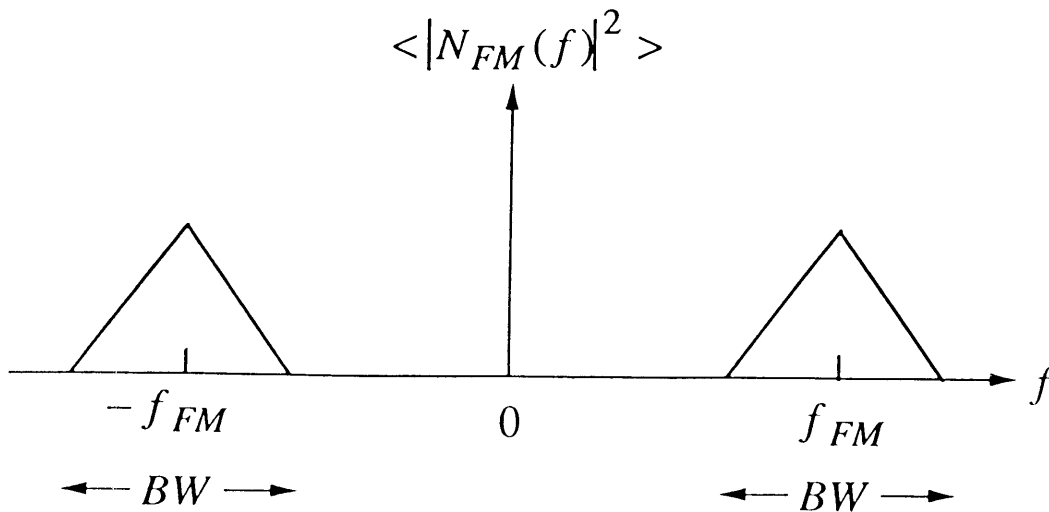


Fig2.8b Modeled FM power spectrum

(2) Due to Automatic Gain Control the sum of localizer power and total interfering power $1.04A_{loc}^{IF2} + A_{intf}^{IF2} + \sum_{i=1}^N A_i^2$ is approximately constant. Therefore the variable localizer amplitude A_{loc}^{IF} can be replaced by the square root of total interfering power $P_{intf} = A_{intf}^{IF2} + \sum_{i=1}^N A_i^2$.

(3) Monte Carlo simulation is carried out for CDI evaluation. Since FM signal is a stochastic process, the spectrum mentioned here refers to the ensemble average of the Fourier transform of waveform in time domain, i.e. average spectrum. The IM spectrum in real radio environment differs from that in experimental condition. In real environment IM interference is the product of three FM signals, therefore the shape of its spectrum is the convolution of three FM spectra. In B1 immunity experiments one FM channels along with two pure carriers are served as input noises, so the shape of IM spectrum is the same as FM spectrum. Because the reproduction of experimental results is the pre-requisite to the theoretical works proposed here, the latter condition is adapted in our model. International Telecommunication Union (ITU) has defined the average power spectrum of an FM channel used in interference immunity experiments on ILS localizer receivers [20](see Figure 2.8a). The FM spectrum in Figure 2.8a has the 20-dB bandwidth 34 KHz. The power of frequency components outside the bandwidth is at most 0.01 times of that at center frequency. For simplicity we could assume that their contribution is negligible. In this thesis the shape of ITU FM power spectrum $S_{FM}(f)$ is approximated as a triangle within bandwidth BW and vanishes out of bandwidth, as in Figure 2.8b. The absolute value of average FM spectrum $H_{FM}(f)$ equals to $\sqrt{S_{FM}(f)}$. Based on average FM power spectrum Monte Carlo simulation on baseband model is possible. The ensemble average and standard deviation of CDI values are functions of total interfering power and IM interfering power.

(4) Baseband stage model should confirm to the ILS localizer receiver standards when there is no interference. First, CDI current is proportional to DDM ($= m_{90} - m_{150}$). If DDM= d corresponds to CDI= $c\mu A$, then DDM= $-d$ corresponds to CDI= $-c\mu A$. Second, at full deflection DDM=0.155 corresponds to CDI current $150\mu A$. Before feeding into noise baseband stage model should be calibrated accordingly.

We use the following procedure to estimate CDI mean and standard deviation:

1. Calibrate the parameters of baseband stage model under signal-only conditions. The conditions needed to be satisfied are that (1) the simulated CDI equal to $150\mu A$ when DDM=0.155; (2) if the simulated CDI value is $c\mu A$ when DDM value is d , then the simulated CDI value will be $-c\mu A$ when DDM value becomes $-d$. 90 Hz filter gain and bandwidth, 150 Hz filter gain and bandwidth, and comparator gain are adjusted accordingly.
2. Choose the appropriate DDM value such that the simulated CDI= $90\mu A$ under signal-only conditions. This is the standard condition under which localizer receiver bench experiments were conducted. For a realistic receiver this DDM value is about 0.093.
3. Pick up a value for the average intermodulation interference power level. Generate a random interference spectrum by using the given average power level and the average power spectrum prescribed in Figure 2.8b.
4. Convert the intermodulation interference from frequency domain to time domain. Incorporate with the localizer component at IF output, $A_{loc}^{IF}[1 + m_{90} \cos(2\pi \cdot 90t) + m_{150} \cos(2\pi \cdot 150t)] \cos(2\pi f_{IF}t)$. Use the resultant temporal signal as baseband input to do the baseband-stage simulation.
5. Carry out different realizations from 3. to 4. Calculate the average and standard deviation of CDI values and other necessary statistical quantities.

6. Pick up different values for average interference power level, repeat 3. to 5. Construct the relationship of CDI mean and standard deviation to interference power level.

2.4.3 Modeling of Envelope Detector

The operation of an envelope detector could be obtained from circuit analysis. The structure of an envelope detector is a full-wave rectifier followed by a low-pass filter. Usually a four-diode bridge is served as rectifier, and a parallel RC circuit is served as low-pass filter. Figure 2.9 illustrates its circuit diagram.

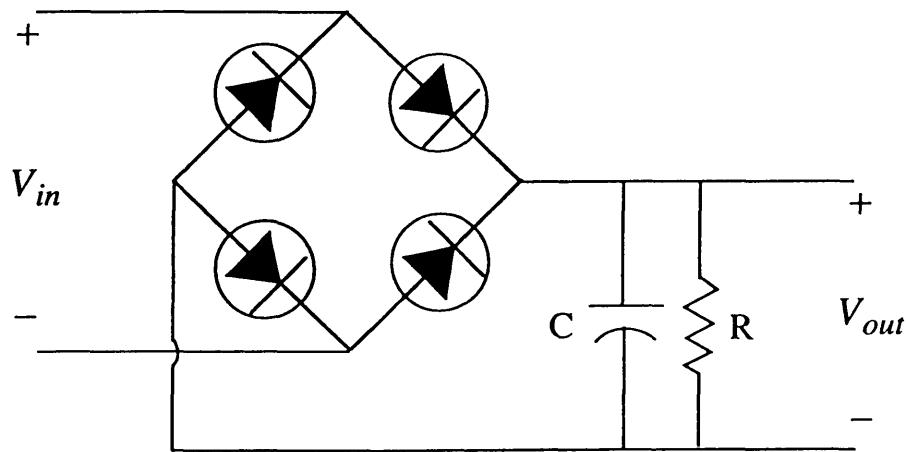


Fig2.9 Envelope detector circuit

Assume D1, D2, D3, D4 are idea diodes. Only ON and OFF states apply to those diodes. For the ON state, the forward diode voltage $V_d = 0$ if the forward diode current $I_d > 0$; for the OFF state the diode current $I_d = 0$ if the diode voltage $V_d < 0$. Then the output is switched between two conditions: when D1/D3 or D2/D4 are ON, the output voltage follows the input voltage; when all diodes are OFF, the output voltage decays exponentially with RC time constant. And the switching is determined by the polarity of current. It is formulated as follows.

$$v_{out}(t) = \begin{cases} v_{out}(t_0) \exp\left(\frac{-(t-t_0)}{RC}\right), & \text{if } v_{out}(t) > |v_{in}(t)| \\ |v_{in}(t)|, & \text{if } \frac{dv_{out}}{dt} + \frac{1}{RC}v_{out} > 0 \end{cases} \quad (2.4.4)$$

The output could be approximated by discretizing continuous time into a series of finite steps:

$$t_n = n\Delta t$$

$$v_{out}(t_n) \approx \begin{cases} v_{out}(t_{n-1}) \exp\left(\frac{-\Delta t}{RC}\right), & \text{if } v_{out}(t_n) > |v_{in}(t_n)| \\ |v_{in}(t_n)|, & \text{if } \frac{(v_{out}(t_n) - v_{out}(t_{n-1}))}{\Delta t} + \frac{1}{RC}v_{out}(t_n) > 0 \end{cases} \quad (2.4.5)$$

2.4.4 Modeling of Final Signal Processing Stage

As indicated in Figure 2.1, the detector output is fed into the 90 Hz and 150 Hz detection blocks simultaneously to retrieve the amplitudes of 90 Hz and 150 Hz components. The output signals from these two blocks are fed into a differential amplifier, hereby generates CDI current. The 90 Hz/150 Hz detection block contains a bandpass filter with central frequency 90/150 Hz and an envelope detector. The envelope detector has been modeled in Section 2.4.3. The bandpass filter is typically designed as a fourth-order Butterworth filter [26]:

$$|H_{base}(f)| = \frac{1}{\sqrt{1 + 1.51 \left(\frac{f_{central}^2 - f^2}{BW \cdot f}\right)^4}} \quad (2.4.6)$$

where $f_{central}$ is its central frequency, and BW is its bandwidth.

Similar to Section 2.4.3, all the signal flow is simulated in discrete level. The simulation processes are arranged in this way:

1. Convert the discrete-time input signal (see (2.4.5)) into frequency-domain signal.
2. Multiply it with 90 Hz bandpass filter response $H_{base}(f)$ (see eqno(2.4.6)).
3. Inverse transform the resultant frequency-domain signal into time domain.
4. Pass through the envelope detector. Use (2.4.5) to evaluate the output.
5. Repeat (2) to (4) for 150 Hz portion.
6. Pass the results obtained from (4) and (5) into a differential amplifier to obtain the difference. Multiply it by a constant gain. Take time average of the result to get CDI output.

2.4.5 Approximation Scheme of IF Envelope Detector

The input of IF envelope detector (denoted by $x_{in}(t)$) contains IF localizer signal and IF noise (denoted by $N_{IM}^{IF}(t)$) with the specific average power spectrum (as indicated in Figure 2.10),

$$x_{in}(t) = A_{loc}^{IF} [1 + m_{90} \cos(2\pi \cdot 90t) + m_{150} \cos(2\pi \cdot 150t)] \cos(2\pi f_{IF}t) + N_{IM}^{IF}(t)$$

The function of envelope detector model is to simulate the output temporal signal $x_{out}(t)$ in response to the input $x_{in}(t)$. As described in Section 2.4.3, the operation of an envelope detector can be numerically simulated by using finite-difference method. The IF envelope detector receives IF localizer signal and noise and converts them into the baseband. In order to avoid under-sampling the sampling rate should be comparable to f_{IF} (or even higher since the interference contains higher frequency components). For a fixed total simulation duration T , the number of time steps for a single realization is $\approx O(T \cdot f_{IF})$. The total simulation duration T is related to the frequency resolution. It should be longer than one period of 90 Hz (≈ 0.011 sec). f_{IF} is in the order of MHz. In sixth-order Chebyshev model it is 30.5 MHz. So the number of time steps, if estimated practically, is about the order of 10^6 . A lot of computation time should be spent on simulating envelope detector.

An approximation scheme can be used to reduce computational complexity of direct simulation on envelope detector. The rationality of this scheme is that by replacing the original IF interference with a baseband interference at input, we can get approximately the same output. And the computational complexity of envelope detector simulation in response to this new input is much lower since the input has a much smaller bandwidth. The method is depicted as follows.

Define a baseband noise $N_{IM}^{base}(t)$ such that

$$N_{IM}^{IF}(t) = N_{IM}^{base}(t) \cdot 2 \cos(2\pi f_{IF}t)$$

The Fourier transform of a time-domain signal $x(t)$ is denoted by $x_F(f)$. It is obvious that the spectrum of baseband noise N_{IM}^{base} is a direct translation of IF noise spectrum.

$$N_{IMF}^{IF}(f) = N_{IM}^{base}_F(f - f_{IF}) + N_{IM}^{base}_F(f + f_{IF}) \quad (2.4.7)$$

Now define a new input $x_{in}^*(t)$ to the same envelope detector. It contains baseband localizer signal and baseband noise,

$$x_{in}^*(t) = A_{loc}^{IF} [1 + m_{90} \cos(2\pi \cdot 90t) + m_{150} \cos(2\pi \cdot 150t)] + N_{IM}^{base}(t)$$

The average power spectrum of N_{IM}^{base} and baseband localizer are demonstrated in Figure 2.10. Denote the envelope detector output in response to $x_{in}^*(t)$ as $x_{out}^*(t)$. Then $x_{out}^*(t) \approx x_{out}(t)$ if the relaxation time of envelope detector is much longer than the period (or the duration when signal level approaches but not exactly equals to original values, i.e. quasiperiod) of $x_{in}(t)^*$. The reason is obvious: $x_{in}^*(t)$ is the envelope of $x_{in}(t)$, and $x_{out}^*(t)$ is the envelope of $x_{in}^*(t)$; if detector's relaxation time is too long to follow the variation of $x_{in}^*(t)$, then the envelope of $x_{in}(t)$'s envelope will be detected at output. Under this approximation, the sampling rate that could recover characteristics of baseband signal $x_{in}^*(t)$ is adequate. Therefore it is in the order of baseband noise bandwidth BW . The number of time steps $\approx O(T \cdot BW)$. Compared with direct simulation, it would save computation time with the ratio $\left(\frac{f_{IF}}{BW}\right)$. The FM bandwidth BW is usually tens of KHz. So the computational complexity is reduced by three orders of magnitude compared to the original scheme. The validity of this approximation scheme could be illustrated by comparing the direct simulation results with approximated simulation results.

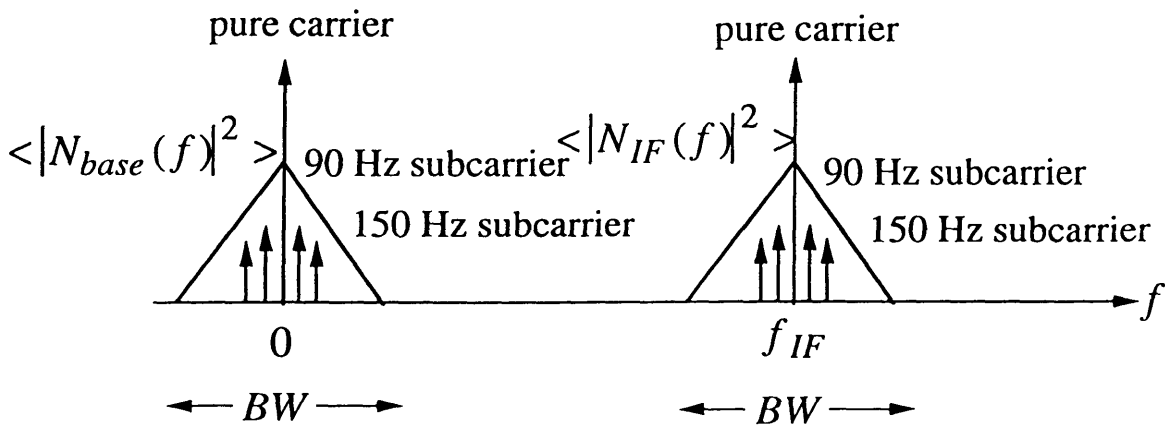


Fig2.10 IF and baseband noise spectrum(one side)

In the following paragraph we conduct numerical simulation on baseband stage (including envelope detector) to show that our approximation scheme is valid. The baseband receiver parameters and other simulation conditions are described as follows:

Receiver Parameters:

IF center frequency : $f_{IF} = 30.5 \text{ MHz}$

IF envelope detector bandwidth: 500 Hz

IF reference voltage level: $V_{ref} = 0.212V$

90/150 Hz filter bandwidth: $BW_{base} = 30 \text{ Hz}$

90/150 Hz filter gain: $A_{90} = 1.0$, $A_{150} = 1.021$

90/150 Hz envelope detector bandwidth: 10 Hz

differential amplifier gain: $A_d = 4.96$

output impedance: $R_o = 1k\Omega$

Simulation Conditions:

noise bandwidth: $BW_N = 64.0 \text{ KHz}$

simulation period $T = 0.1 \text{ sec}$

number of IF noise levels between and 100% noise: 50

number of samples for IF-envelope-detector simulation: 3072000

number of samples for baseband simulation: 1024

Table 2.1 is the simulated CDI output for zero-noise condition. Figure 2.11 demonstrates the simulated CDI values under different IF noise levels for a single realization. The symbol 'a' represents the results from direct simulation of envelope detector, while the symbol 'x' represents the results from approximation scheme of envelope detector (1024 samples for one simulation). The approximation method obviously could reproduce exact simulation results. Figure 2.12 is CDI mean and standard deviation by using the approximation scheme for 300 realizations. The average is desensitized with increasing noise level, while the standard deviation increases with noise level. After performing the Monte Carlo simulation on baseband stage, we could link it with the deterministic frequency selection stage model and carry out a complete simulation on the whole receiver.

DDM	0.093	-0.093	0.155	-0.155
CDI(μA)	90.23	-90.41	150.74	-149.85

Table2.1 Simulated CDI for zero-noise conditions

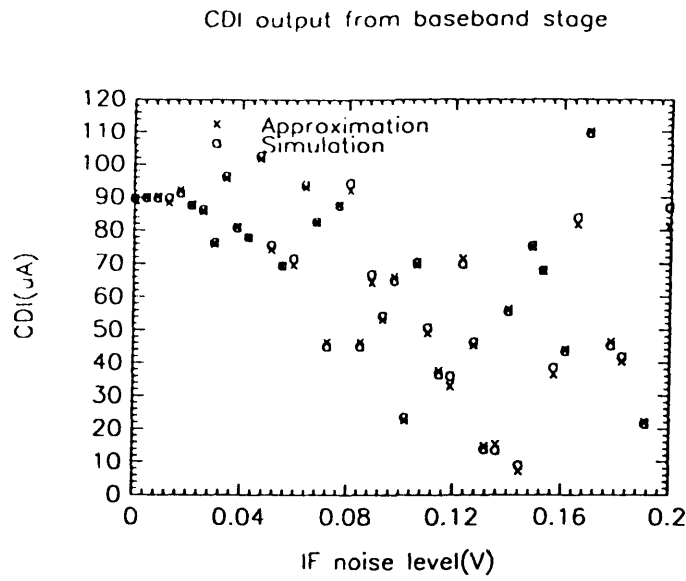


Fig2.11 CDI output based on simulated and approximated envelope detector

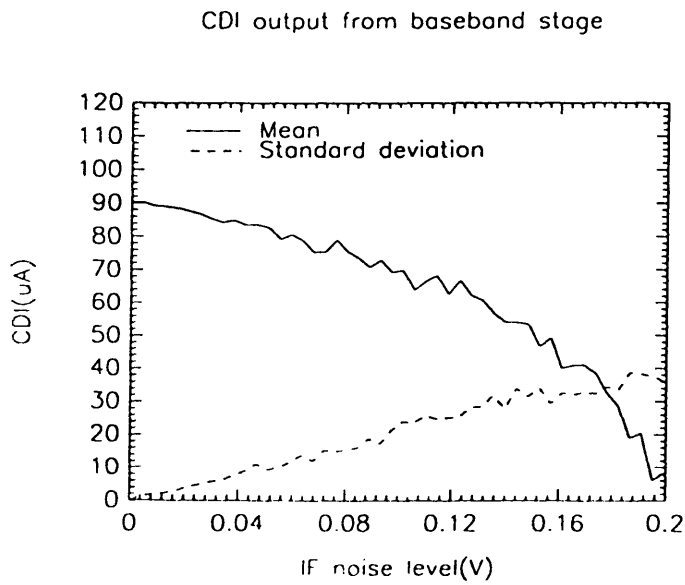


Fig2.12 CDI mean and standard deviation

Chapter 3

Model Synthesis

3.1 EXPERIMENTS FOR ILS RECEIVER INTERFERENCE

In order to understand ILS localizer receiver's susceptibility to interference, Federal Aviation Administration (FAA) and other civil aviation authorities conducted a series of bench tests over different kinds of receivers. The focus is to measure the 'threshold' of input interfering power; that is, for a certain localizer power level and a set of interfering frequencies, to what extent the input interfering power should reach in order to cause 'intolerable' CDI error. FAA and International Telecommunication Union (ITU) have developed different regression formula to describe these experimental data in different perspective. These formula serve as reference of theoretical model proposed in Chapter 2: simulation results from a correct model should fit experimental data.

The standard experimental procedures for two-frequency intermodulation (B1) interference of ILS localizer receivers could be outlined as follows. Figure 3.1 is the corresponding equipment setup for two-frequency B1 experiments.

1. Use localizer simulator to generate localizer signal with chosen carrier frequency f_{loc} and power level (e.g. -86 dBm). Pick up a type of localizer receiver set. Inject localizer signal into localizer receiver and read CDI current value. Adjust DDM value until 90 μA CDI current is read.

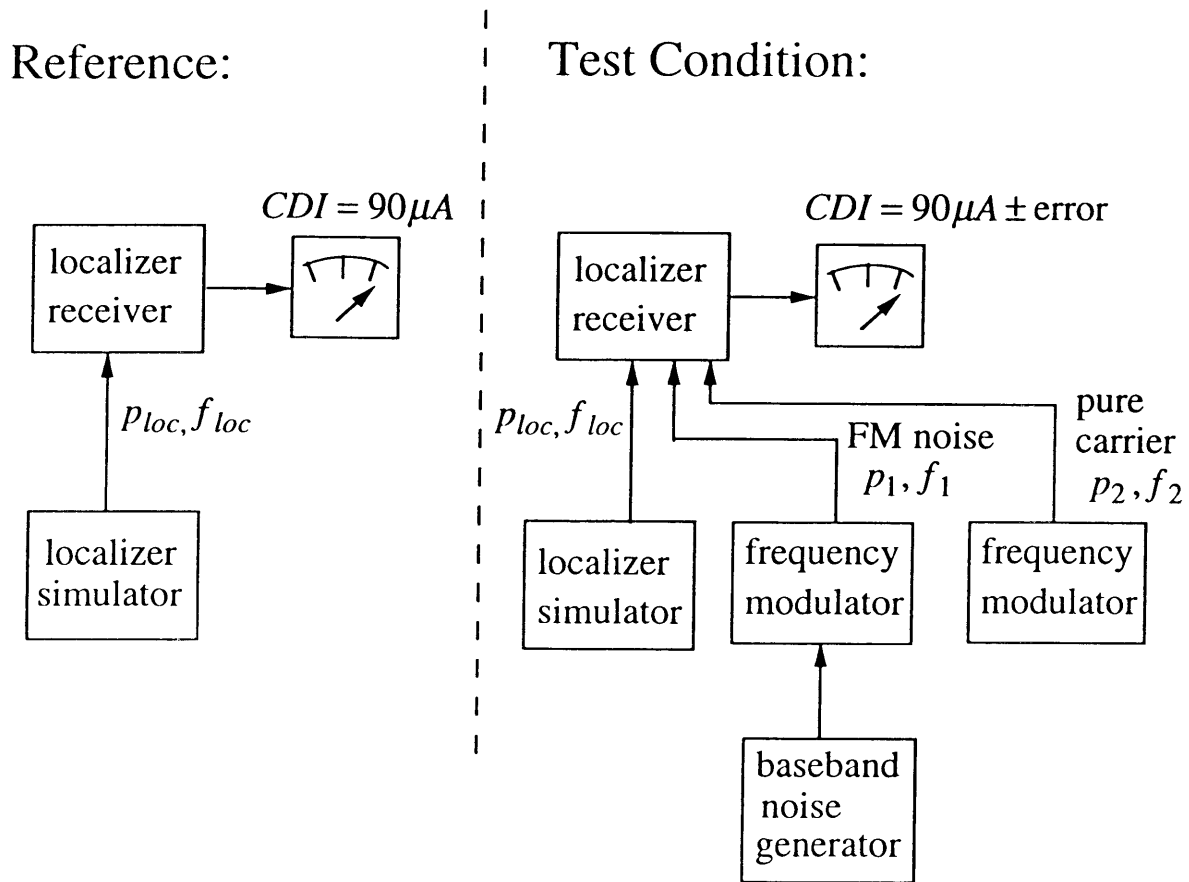


Fig3.1 Experimental setup for ILS B1-interference tests

2. Use noise simulator and frequency modulator to generate FM noise with carrier frequency f_1 . The other interference component is FM without audio message (i.e. a pure carrier) with chosen frequency f_2 . f_1 and f_2 are chosen to satisfy intermodulation condition $2f_1 - f_2 = f_{loc}$. Feed both components into receiver. Their power levels are set equal all the time. The level is called equisignal level.

3. At a fixed interference power level, CDI output is not always at constant level but fluctuates with time. Write down all the CDI sample values at that level. Do statistical analysis on those sample data to see if the statistical outcomes meet the threshold condition. If not, increase input interference power level by 1-dB step and repeat the process until threshold condition is reached. The corresponding equisignal level is defined as the 'threshold' of input interference power. Write down the threshold value. The threshold conditions for different models are different. For AAM the threshold is defined as the condition when 10% of CDI sample values fall out of $(90 \pm 9)\mu A$ (i.e. $> 99\mu A$ or $< 81\mu A$). For ITU model if the CDI standard deviation exceeds $2.25 \mu A$ then threshold is reached.

4. Change different FM channels f_1 f_2 that satisfy intermodulation condition. Carry out 2 to 3. Get threshold values corresponding to different frequency combinations.

5. Change localizer power to different levels (e.g. -49dBm, -67dBm). Repeat 1 to 4.

6. Repeat procedures 1 to 5 for different types of localizer receiver sets.

IM threshold varies with input interfering frequencies. In two-frequency B1 case IM threshold is a function of f_1 and f_2 . However, casting the experimental outcome into multi-dimensional domain would make regression analysis more complicated. From statistical analysis of experimental data, it was found that the most relevant single variable to IM threshold is the product of separation between localizer and interfering frequencies $(f_{loc} - f_1)(f_{loc} - f_1)(f_{loc} - f_2)$. So the FAA and ITU represent IM threshold as a dependent variable of only one independent parameter which measures the frequency separation. For two-frequency IM case it is defined this way:

AAM Model:

$$g_a = \log |(f_{loc} - f_1)(f_{loc} - f_1)(f_{loc} - f_2)| \quad (3.1.1)$$

ITU Model:

$$g_{it} = \log \| \text{Max}(1.0, f_{loc} - f_1) \text{Max}(1.0, f_{loc} - f_1) \text{Max}(1.0, f_{loc} - f_2) \| \quad (3.1.2)$$

where all frequencies are in MHz unit.

The experimental procedure for three-frequency intermodulation interference is almost the same as two-frequency except three different noise sources with frequencies f_1 , f_2 , f_3 (one is FM, the other two are pure carriers) satisfying intermodulation condition are fed into localizer receiver. The definition of g for AAM and ITU models are similar to (3.1.1) and (3.1.2) except an f_1 is replaced by f_3 .

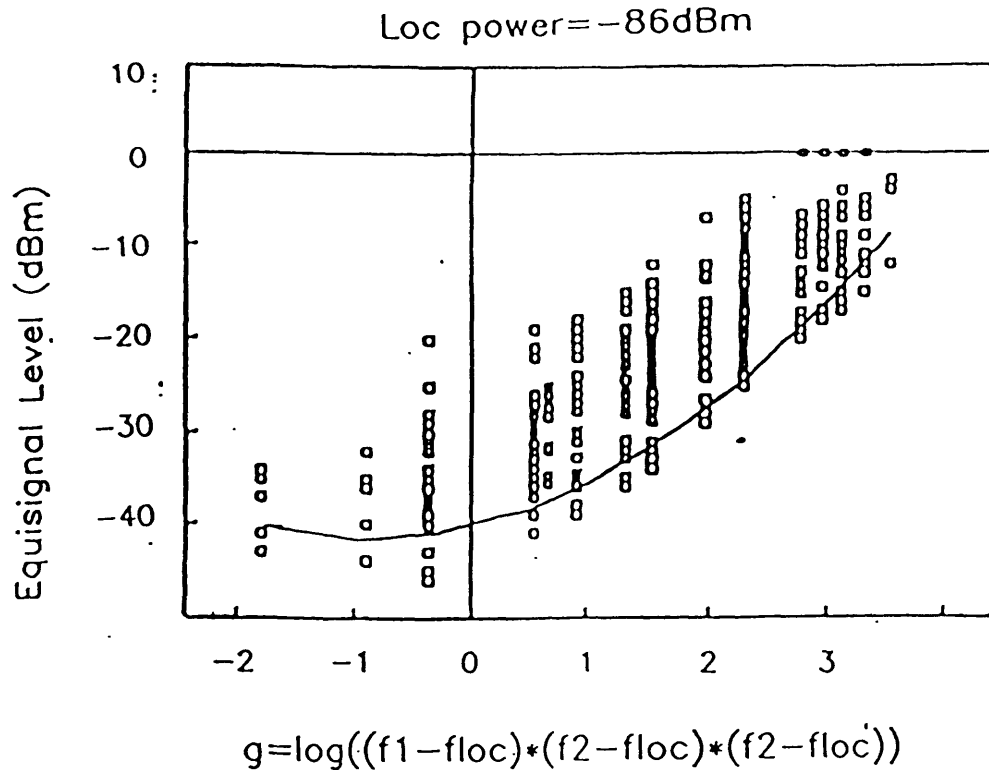


Fig3.2 FAA intermodulation threshed test results [9]

Figure 3.2 demonstrates FAA bench measurement data of two-frequency B1 interference at a specific localizer power (-86dBm). Each tiny square represents one data point. The solid line is the regression curve fitting 5% worst data points. The samples were taken after measuring 25 kinds of ILS receivers at different conditions [9]. Different data points at same g value represent different kinds of receivers. Among these data points the ones with lowest threshold values are of interest since they more or less reflect the worst case of current ILS receivers' interference immunity. In FAA's AAM model the quadratic regression formula reflecting the 5% worst experimental results are described [9]. Notice that AAM experiment results were available for localizer power = -86dBm and -49dBm. Therefore -86dBm and -49dBm formula were derived from empirical data. The conditions in between (i.e. $-86dBm < p_{loc} < -49dBm$) could be interpolated accordingly.

AAM Two Frequencies:

$$Th(g_a, -86) = -40.2590 + 2.9728g_a + 1.6895g_a^2 \quad (3.1.3)$$

$$Th(g_a, -49) = -18.1980 + 2.0070g_a + 1.0596g_a^2 \quad (3.1.4)$$

$$Th(g_a, p_{loc}) = \frac{1}{37}(Th(g_a, -49) - Th(g_a, -86))(g_a + 86) + Th(g_a, -86) \quad (3.1.5)$$

AAM Three Frequencies:

$$Th(g_a, -86) = -40.1634 + 2.1977g_a + 1.5668g_a^2 \quad (3.1.6)$$

$$Th(g_a, -49) = -18.9296 + 1.0941g_a + 1.2215g_a^2 \quad (3.1.7)$$

$$Th(g_a, p_{loc}) = Th(g_a, -86) + \frac{1}{37}(Th(g_a, -49) - Th(g_a, -86))(g_a + 86) \quad (3.1.8)$$

The unit of $Th(.,.)$ and p_{loc} is dBm. g_a is calculated from (3.1.1)

ITU model has different regression formula [3]. The equisignal threshold is linear with both g and localizer power. The dependence of localizer power is also included in the formula.

ITU Two Frequencies:

$$Th(g_{it}, p_{loc}) = \frac{28}{3}g_{it} - 51 + \frac{p_{loc}}{3} \quad (3.1.9)$$

ITU Three Frequencies:

$$Th(g_{it}, p_{loc}) = \frac{28}{3}g_{it} - 53 + \frac{p_{loc}}{3} \quad (3.1.10)$$

The unit of $Th(.,.)$ and p_{loc} is dBm. g_{it} is calculated from (3.1.2)

3.2 MODEL SYNTHESIS-INVERSION OF RECEIVER PARAMETERS

Chapter two gives a detailed description of ILS generic receiver model. This model is generic in the sense that it is characterized by a set of receiver parameters. The receiver parameters are listed below:

Frequency Selection Stage:

Front End: equivalent input impedance R_{in}

RF: A_{RF}^{pre} , $H_{RF}^{pre}(f)$, K_1^{RF} , K_3^{RF} , A_{RF}^{post} , $H_{RF}^{post}(f)$

Mixer: K_2^{Mix} , K_4^{Mix}

Local oscillator output: frequency f_{osc} , amplitude A_{osc}

IF: $H_{IF}^{pre}(f)$, K_1^{IF} , K_3^{IF} , $H_{IF}^{post}(f)$

IF output voltage level: V_0

Baseband Stage:

IF envelope detector: time constant t_{IF}

90/150 Hz Bandpass filter: bandwidth BW_{90} / BW_{150} , gain A_{90} / A_{150}

90/150 Hz envelope detector: time constant t_{90} / t_{150}

differential amplifier: gain A_d , impedance R_d

In this model the determination of baseband-stage parameters is based on the criterion mentioned in Section 2.4.2: baseband simulation model should satisfy the proportional condition — if $DDM=d$ corresponds to $CDI=c\mu A$ then $DDM=-d$ corresponds to $CDI=-c\mu A$; as well as the maximal deviation condition — $DDM=0.0155$ corresponding to $150\mu A$ CDI current. The former could be achieved by adjusting the ratio BW_{90}/BW_{150} and A_{90}/A_{150} . The later could be achieved by adjusting others. However, the two conditions do not uniquely determine the value of every baseband parameter. In realistic situation these values, depending on different circuit designs, vary from one to another type of ILS receivers. We assign these values such that they approximately fit the scale of real receiver circuits.

Unlike baseband parameters which are determined by the response to pure localizer signal, frequency-selection stage parameters could be inverted from experimental results. Setting the input interference power at the equisignal threshold, we can simulate the receiver response. The total (third-order)IM power depends on RF filters response A_{RF}^{pre} , $H_{RF}^{pre}(f)$, A_{RF}^{post} , $H_{RF}^{post}(f)$, as well as RF amplifier (third-order) nonlinearity $\frac{K_3^{RF}}{K_3^{RF}}$ and balanced mixer (fourth-order) nonlinearity $\frac{K_4^{Mix}}{K_2^{Mix}}$. Note the local oscillator output voltage A_{osc} and input impedance R_{in} also have effects since the former is related to the value of mixer nonlinearity (see (2.3.7)) and the latter transfers power level into voltage level. The regression curves of AAM, ITU and ICAO models provide the lower bound for the IM interference immunity of ILS receivers. If we could find out a set of parameter values that fit simulation results with

empirical regression curves, then these values are considered a characterization of ILS localizer receivers. The set of parameters corresponding to AAM regression curves is the representation of so-called “AAM receiver”, and the set corresponding to ITU or ICAO regression curves is the representation of so-called “ITU receiver” or “ICAO receiver”.

This inverse problem could be formulated as a least-square optimization problem. Parameters are denoted by a vector $\mathbf{b} = (b_1, b_2, \dots, b_M)$. Input quantities are denoted by $\mathbf{x} = (g, p_{loc})$. There are N different sampling points related to N different input conditions $\mathbf{x}_1, \mathbf{x}_2, \dots, \mathbf{x}_N$. The threshold value corresponding to input \mathbf{x}_i is y_i^{ref} from regression formula, and is y_i from theoretical model. y_i is a function of receiver parameters, $y_i = y_i(\mathbf{b})$. The inverse problem is to find out a parameter vector \mathbf{b}_0 such that the distance between empirical and theoretical results, defined as $\sum_{i=1}^N |y_i^{ref} - y_i(\mathbf{b}_0)|^2$, is minimal. In another word, let $\mathbf{Y} = (y_1, y_2, \dots, y_N)$, $\mathbf{Y}^{ref} = (y_1^{ref}, y_2^{ref}, \dots, y_N^{ref})$, the problem is to find out \mathbf{b}_0 such that the objective $\|\mathbf{Y}(\mathbf{b}_0) - \mathbf{Y}^*\|_2$ is minimal.

The input variable g is actually a specification of input interfering frequencies. For two-frequency intermodulation case, the input frequencies are uniquely determined by g , for three-frequency intermodulation case they are not uniquely determined. The inversion scheme adopts regression formula of two-frequency B1 as reference to inverse receiver parameters. The parameters to be inverted and input conditions designated in our inversion scheme are depicted below:

Inverted Parameters:

$$R_{in}, A_{RF}^{pre}, H_{RF}^{pre}(f), K_4^{Mix}/K_2^{Mix}, A_{osc}$$

$$K_3^{RF}/K_1^{RF}(p_{loc} = -86dBm), K_3^{RF}/K_1^{RF}(p_{loc} = -67dBm),$$

$$K_3^{RF}/K_1^{RF}(p_{loc} = -49dBm), K_4^{Mix}/K_2^{Mix}, A_{osc}$$

Input conditions: 10 sets of FM channels whose g values are approximately equally spaced between -2.0 and 3.35, $p_{loc} = -86\text{dBm}$, -67dBm and -49dBm .

Note certain assumptions are imposed on pre-filter response $H_{RF}^{pre}(f)$. The peak is assumed to lie exactly at localizer frequency, i.e. the filter is tunable. In addition, filter response is assumed symmetric with respect to center (localizer) frequency. Even though several exceptions still exist, these two properties are common for contemporary receivers. In order to implement optimization algorithm, the continuous filter response function is discretized into 17 levels between 87.5 MHz and center frequency. The RF-amplifier nonlinearity K_3^{RF}/K_1^{RF} changes with different input localizer power. It is consistent with experimental results [7].

Several algorithms are available for least-square optimization. Most of them are iterative. The procedures for an iterative optimization algorithm are as follows. (1) We start from an initial guess \mathbf{b} , get theoretical output \mathbf{Y} , compute $\|\mathbf{Y} - \mathbf{Y}^{\text{ref}}\|_2$. (2) If the distance between theoretical output and reference is either larger than prescribed tolerance or allowable for further improvement, then we add \mathbf{b} by a quantity $\delta\mathbf{b}$ which is determined by algorithm, repeat (1) and (2). Among the optimization algorithms Newton-Raphson and steepest-descent methods are the most common two. In the former method $\delta\mathbf{b}$ is equivalent to the first-order correction, while in the latter one $\delta\mathbf{b}$ is selected such that the changing rate of output \mathbf{Y} is largest. Newton's method converges rapidly if a good starting point is given, but for poor starting points it doesn't behave well to converge. Steepest-descent method, on the contrary, is expected to converge for poor starting points, but requires a lengthy solution time [18]. The inversion scheme adopts a method which take advantage of both extremes: Marquardt's algorithm. In this method the modification vector $\delta\mathbf{b}$ is determined in this way [18]:

$$[\mathbf{A}^T \mathbf{A} + \lambda \mathbf{I}] \delta\mathbf{b} = \mathbf{A}^T (\mathbf{Y} - \mathbf{Y}^{\text{ref}}) \quad (3.2.1)$$

A is an $N \times M$ matrix with element $A_{ij} = \frac{\partial Y_i}{\partial b_j}$. A^T is A 's transpose matrix. I is an $N \times N$ identity matrix. λ is a correction factor. It can be shown that when $\lambda = 0$ Marquardt's algorithm becomes Newton's method, when $\lambda = \infty$ it becomes steepest-descent method. Thus in Marquardt procedure the initial values of λ are large and will decrease toward zero as the optimum is approached.

Figure 3.3 is a diagrammatic representation of model synthesis procedures. By the accomplishment of these procedures we should be able to invert AAM, ITU and ICAO receivers.

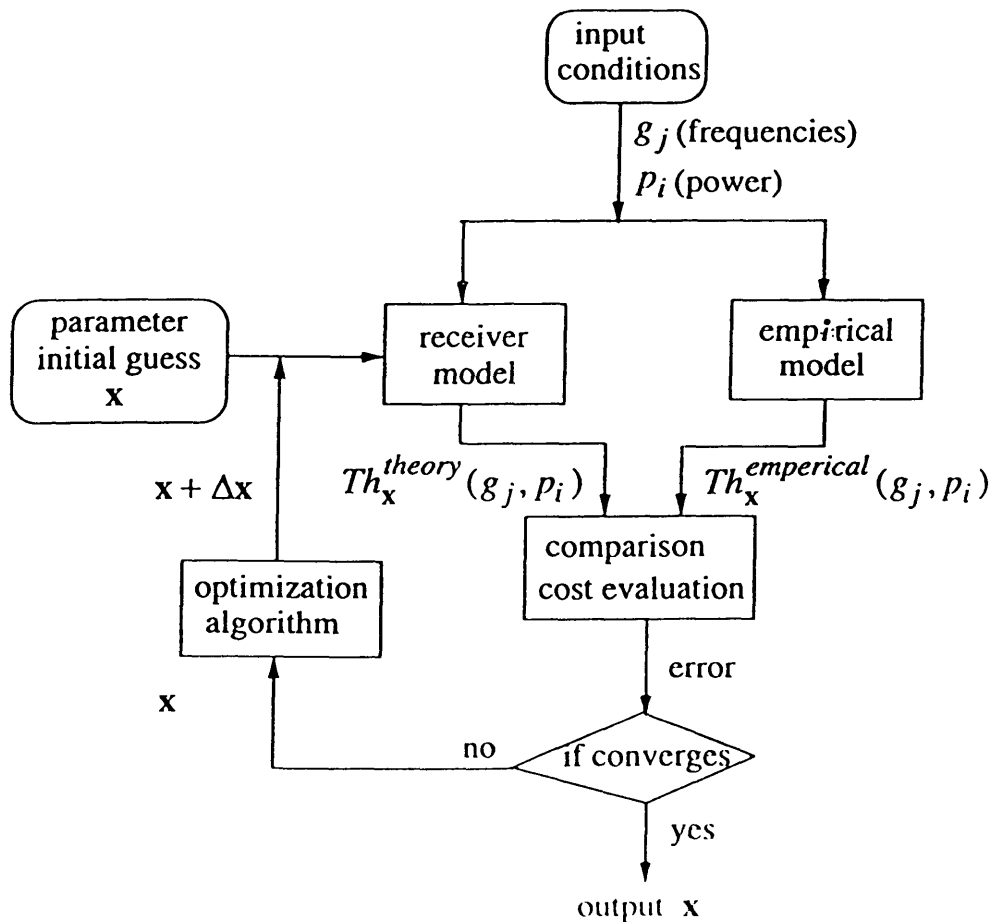


Fig3.3 Parameter inversion procedures

3.3 INVERTED RECEIVERS AND THRESHOLD CURVES

The inverted results are demonstrated as follows. Figure 3.4 and 3.5 are pre-filter's frequency responses of inverted AAM and ITU receivers. Table 3.3 lists the values for the other inverted AAM and ITU receiver parameters. These parameter values are obtained by optimizing simulation results to empirical data for two-frequency regression curves at localizer power levels -86dBm, -67dBm and -49dBm.

Figure 3.6 and 3.8 demonstrate the simulated as well as regression two-frequency B1 threshold curves for AAM and ITU models. If the derived model is self-consistent, the simulation results should also fit empirical data well for other intermodulation conditions. Figure 3.7 and 3.9 demonstrate the simulated as well as regression three-frequency B1 threshold curves for AAM and ITU models. Both two-frequency and three-frequency curves represent finite numbers of frequency combinations. The pairs chosen for two-frequency and three-frequency intermodulation are listed in Table 3.1 and 3.2. The localizer frequency is 108.1 MHz.

As indicated in Figure 3.6 and 3.7, the AAM simulation results deviate more from regression curves when interfering frequencies are close to localizer frequency. From the quadratic regression formula the value increases as frequency separation decreases in this region. On the other hand, receiver model predicts monotonically decreasing when filter responses are monotonic. This discrepancy, in addition to the incompleteness of receiver model or inversion scheme, may be derived from the way AAM empirical formula are developed. AAM formula correspond to the regression of performance among 5% worst receivers. However, the numbers of receivers under test are not all the same for different frequency pairs. There are fewer data points when g is extremely low or high (see Figure 3.2). The 5% lowest data points at low g -values (e.g. $g < -1.0$ in Figure 3.2) may not represent the same kinds of receivers as those at normal g -values. Their threshold equisignal levels at higher g -values may be higher than 5% worst cases.

f_1 (MHz)	107.9	107.7	107.5	107.3	107.1
f_2 (MHz)	107.7	107.3	106.9	106.5	106.1

f_1 (MHz)	106.5	105.5	103.9	101.5	98.1
f_2 (MHz)	104.9	102.9	99.7	94.9	88.1

Table3.1 Intermodulation frequencies(two frequencies)

f_1 (MHz)	107.9	107.9	107.9	107.9	107.7
f_2 (MHz)	107.7	107.5	106.7	106.1	105.3
f_3 (MHz)	107.5	107.3	106.5	105.9	104.9

f_1 (MHz)	107.3	105.9	104.3	102.7	102.1
f_2 (MHz)	104.7	103.9	103.5	100.5	94.1
f_3 (MHz)	103.9	101.7	99.7	95.1	88.1

Table3.2 Intermodulation frequencies(three frequencies)

Model	AAM	ITU
$R_{in} (K\Omega)$	82.22	99.91
A_{RF}^{pre}	0.3	0.8
$K_3^{RF} / K_1^{RF} (-86dBm)$	1.266	1.333
$K_3^{RF} / K_1^{RF} (-67dBm)$	0.949	1.167
$K_3^{RF} / K_1^{RF} (-49dBm)$	0.522	1.000
A_{isc}	0.283	0.600
K_4^{mix} / K_2^{mix}	0.310	0.259

3

Table3.3 Inverted receiver parameters

AAM RF Filter(Center=108.1MHz, BW=1.05MHz)

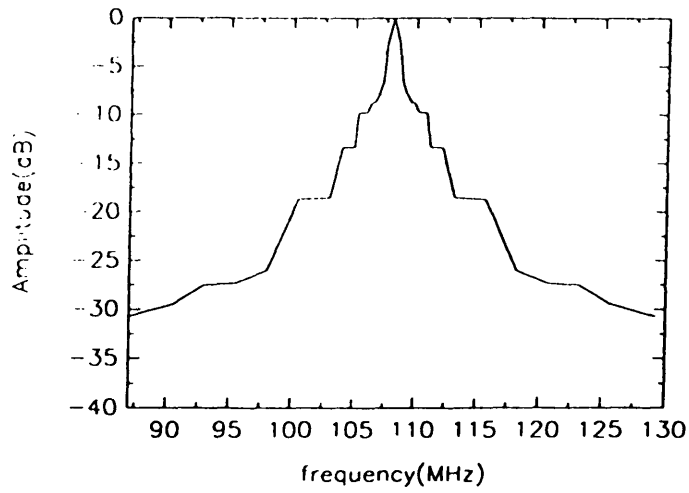


Fig3.4 Inverted AAM RF pre-filter response

ITU RF Filter(Center=108.1MHz, BW=1.36MHz)

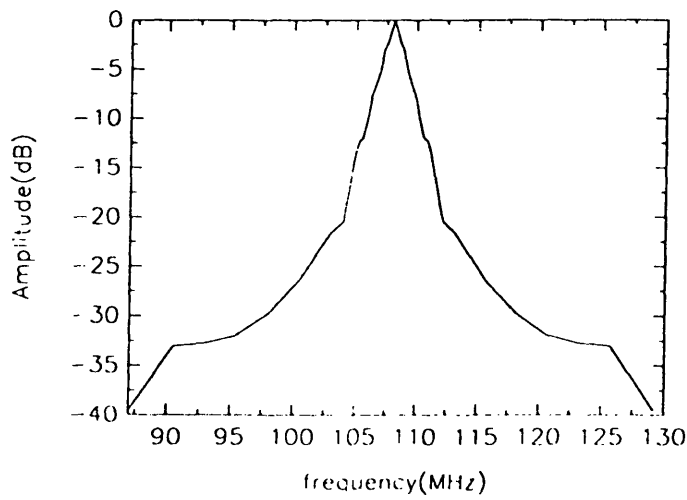


Fig3.5 Inverted ITU RF pre-filter response

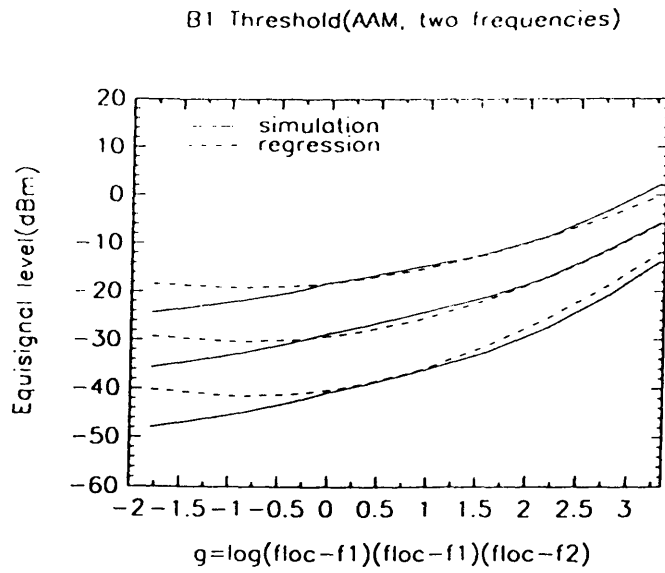


Fig3.6 AAM two-frequency B1 curves

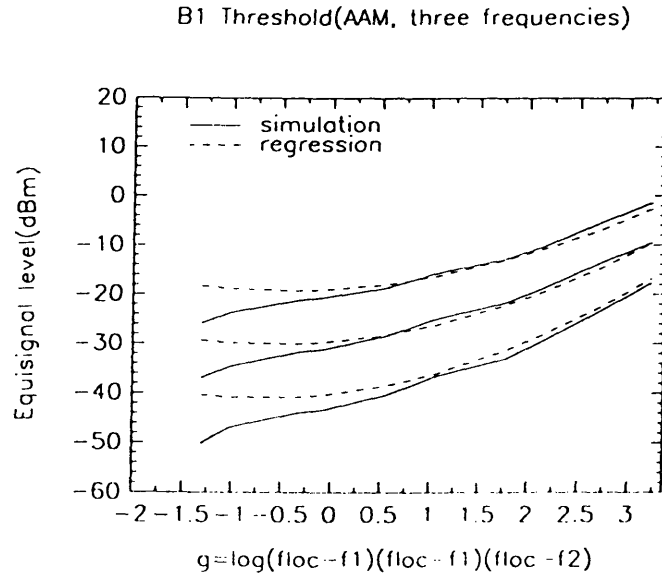


Fig3.7 AAM three-frequency B1 curves

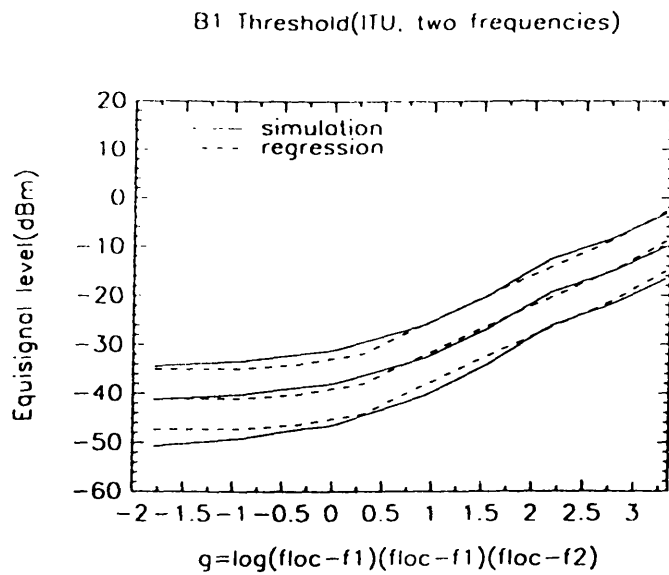


Fig3.8 ITU two-frequency B1 curves

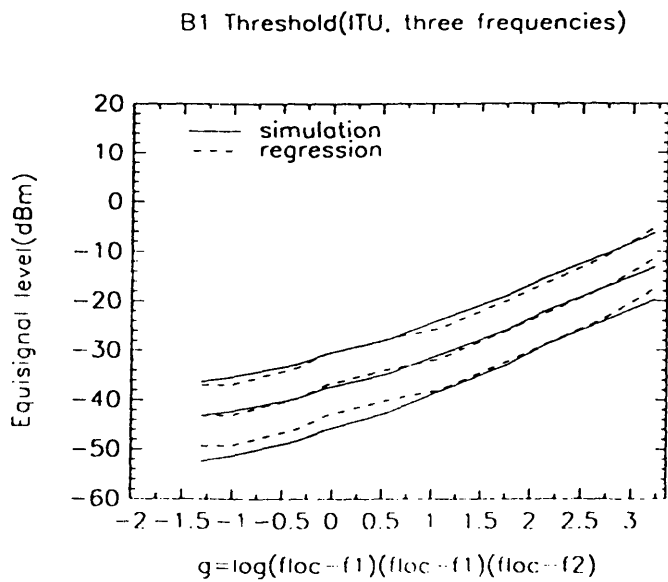


Fig3.9 ITU three-frequency B1 curves

Chapter 4

Model Extension

4.1 DESIGNING THE FUTURE RECEIVERS

AAM and ITU models are the phenomenological descriptions of the ILS receivers on the market. In order to maintain the safety in a “noiser” radio environment a future standard for immunity of ILS receivers was envisioned by the aviation authorities in different countries. Through the International Civil Aviation Organization (ICAO) it was proposed that international carrier fleet are required to conform to a new standard specified by ICAO document Annex 10. This new standard is to be phased in between July 1995 and July 1998. One utility of the inversion scheme in Section 3.2 is to help designing the receivers that fulfill ICAO standard. The values of parameters inverted from ICAO standard can be used as a reference in designing the RF filters, RF amplifiers and mixers of future ILS receivers.

The threshold criterion for ICAO is similar to AAM: interference reaches the level when 10% of CDI sample values fall out of $(90 \pm 7.5)\mu A$. The definition of g in ICAO model for two-frequency intermodulation is

ICAO Model

$$g_{ic} = \log \left| \frac{\text{Max}(0.4, 108.1 - f_1)}{0.4} \frac{\text{Max}(0.4, 108.1 - f_1)}{0.4} \frac{\text{Max}(0.4, 108.1 - f_2)}{0.4} \right| \quad (4.1.1)$$

where all frequencies are in MHz unit.

Three-frequency g is similarly defined where an f_1 is replaced by f_3 .

ICAO curves are similar to their counterparts of ITU regression curves:

ICAO Two Frequencies:

$$Th(g_{ic}, p_{loc}) = \frac{20}{3}g_{ic} + 12.625467 + \frac{p_{loc}}{3} \quad (4.1.2)$$

ICAO Three Frequencies:

$$Th(g_{ic}, p_{loc}) = \frac{20}{3}g_{ic} + 10.625467 + \frac{p_{loc}}{3} \quad (4.1.3)$$

Figure 4.1 is pre-filter's frequency responses of inverted ICAO receiver. Table 4.1 lists the values for the other inverted ICAO receiver parameters. Notice that compared with Table 3.3 ICAO standard could be achieved by desensitizing RF input 26.03 dB with respect to ITU. If we don't resort to this approach but only to sharpen the filter response or to lessen the coefficient of third-order nonlinearity or to both we could still get ICAO receiver. But the filter or amplifier would go far beyond the realizable ranges. Therefore from an engineering point of view RF input desensitization is a sensible design for the fulfillment of higher interference-immunity standard. The reason for it is obvious. Suppose the input localizer level is A_{loc} , and input noise levels for three channels are N_1 , N_2 , N_3 (all in dB scale). The intermodulation level would be $N_1 + N_2 + N_3$ (filter effect). Now the RF input is desensitized by a coefficient A , then localizer level becomes $A_{loc} - A$, while the intermodulation level becomes $N_1 + N_2 + N_3 - 3A$ (filter effect). The $\left(\frac{S}{N}\right)$ ratio improves $2A$ than original one. So intermodulation interference is better suppressed.

Figure 4.2 demonstrates the simulated as well as regression two-frequency BI threshold curves for ICAO model. Figure 4.3 demonstrates the simulated as well as regression three-frequency BI threshold curves for ICAO model. The input frequency pairs chosen for two-frequency and three-frequency intermodulation are same as those in Table 3.1 and 3.2. The localizer frequency is 108.1 MHz.

Model	ICAO
$R_{in} (K\Omega)$	82.22
A_{RF}^{pre}	0.04
$K_3^{RF} / K_1^{RF} (-86dBm)$	1.266
$K_3^{RF} / K_1^{RF} (-67dBm)$	0.949
$K_3^{RF} / K_1^{RF} (-49dBm)$	0.522
A_{osc}	3.283
K_4^{mix} / K_2^{mix}	0.310

Table4.1 Inverted ICAO receiver parameters

ICAO RF Filter(Center=108.1MHz, BW=1.04MHz)

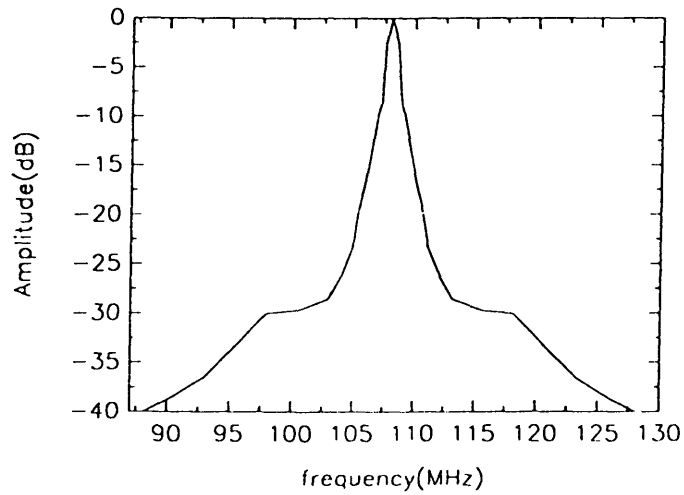


Fig4.1 Inverted ICAO RF pre-filter response

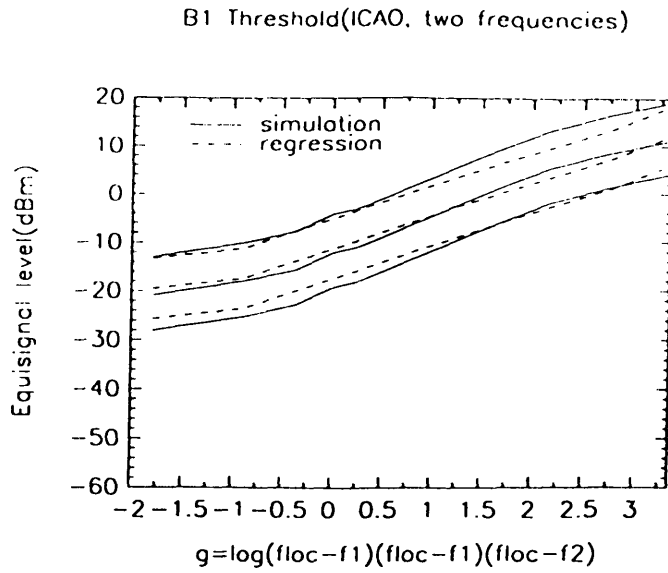


Fig4.2 ICAO two-frequency B1 curves

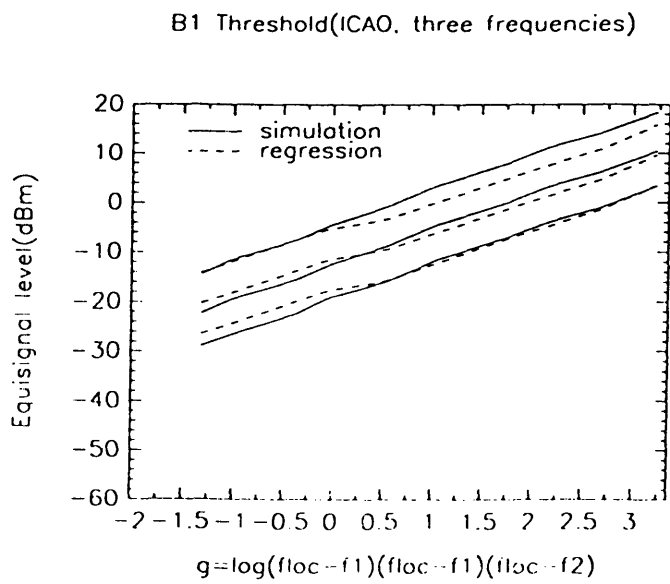


Fig4.3 ICAO three-frequency B1 curves

4.2 PURE-CARRIER INTERMODULATION INTERFERENCE

The extent of pure-carrier intermodulation interference is also of concern to the aviation communities. In order to certify a new receiver radio interference immunity needs to be treated on pure-carrier noise as well as FM noise. It is observed that intermodulation interference from pure carrier might be more serious than that from FM. The simulation procedures are exactly the same as those of Section 4.2 except the noise spectrum mentioned in Section 2.4.2 is replaced by a single component. Notice even though pure carrier, unlike FM noise, has a deterministic spectrum, Monte Carlo simulation is still required since the relative phase of noise carrier with respect to localizer carrier is a random variable. Figure 4.4, 4.5 and 4.6 compare the two-frequency threshold curves for pure-carrier noise with those for FM noise. Even though the total power of pure carrier locates out of both the 90 Hz and 150 Hz filter passband, this comparison shows that pure-carrier intermodulation interference is at least as serious as FM intermodulation interference. In AAM and ITU models the former ones are even more serious. It is because the impact of interference cannot be comprehend as direct 'leaking' to baseband stage but involves the envelope extraction which in itself is a nonlinear operation.

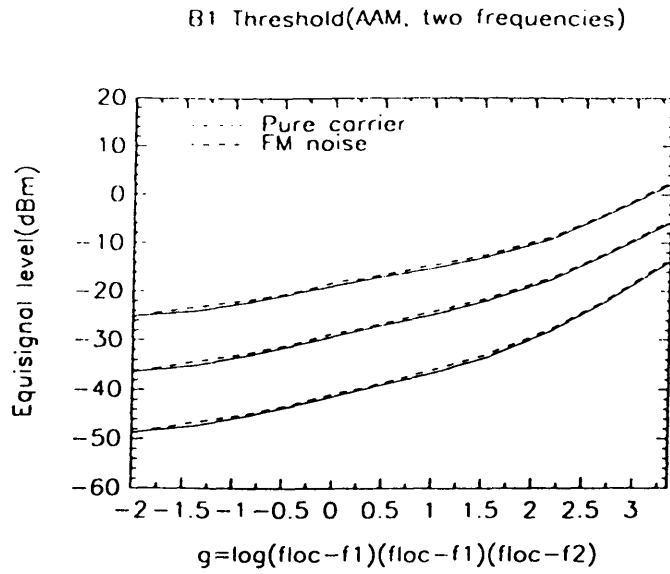


Fig4.4 Comparison of pure-carrier interference with FM interference: AAM model

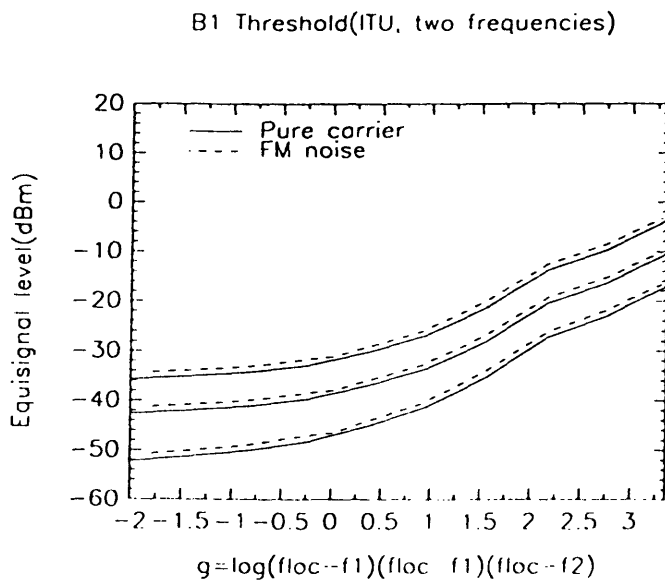


Fig4.5 Comparison of pure-carrier interference with FM interference: ITU model

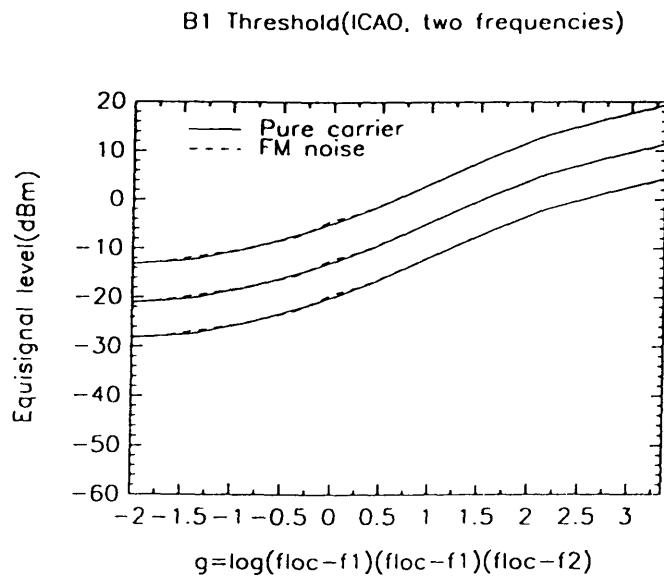


Fig4.6 Comparison of pure-carrier interference with FM interference: ICAO model

4.3 CALCULATION OF COURSE DEVIATION CURRENT

The function of this model is to calculate CDI under various interference conditions, including both threshold and non-threshold. By using this model as a tool the simulation on aircraft landing process could be carried out.

Since the noise assumed in this model is stochastic, CDI value is also non-deterministic. We could simulate its statistical behavior. Take AAM receiver as an example. Figure 4.7 is the simulated AAM threshold curve at localizer power -86 dBm and frequency 108.1 MHz. Icons 'A', 'B', and 'C' represent over-threshold (noise power -37 dBm), threshold (noise power -39 dBm) and under-threshold (noise power -41 dBm) conditions when a specific intermodulation pair is selected ($f_1 = 107.1$ MHz, $f_2 = 106.1$ MHz). Figure 4.8 to Figure 4.10 represent CDI distribution under condition 'A', 'B' and 'C'. The number of realizations is 200.

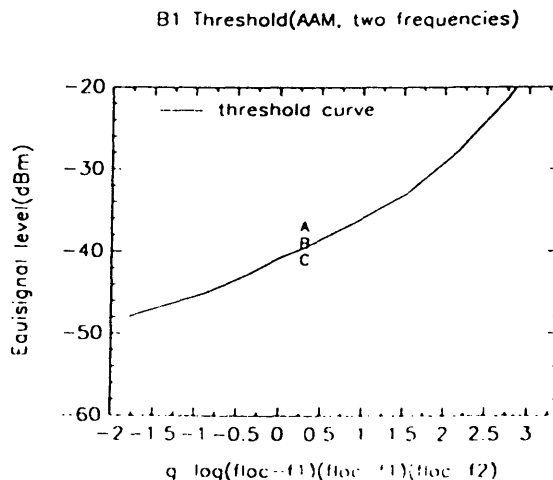


Fig4.7 Specification of over-threshold, threshold and under-threshold conditions

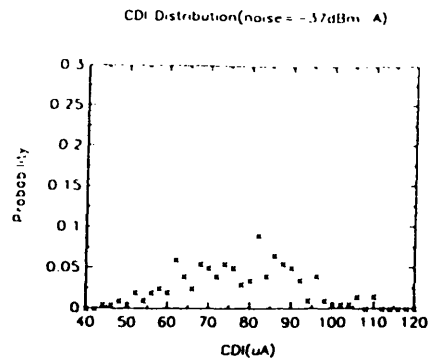


Fig4.8 CDI distribution(over-threshold): mean= $78.01 \mu A$, deviation= $13.66 \mu A$

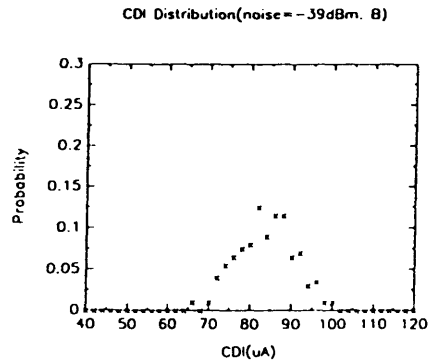


Fig4.9 CDI distribution(threshold): mean= $84.77 \mu A$, deviation= $6.90 \mu A$

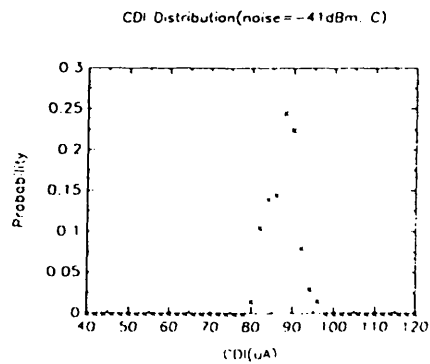


Fig4.10 CDI distribution(under-threshold) mean= $88.53 \mu A$, deviation= $3.56 \mu A$

Chapter 5

Conclusion

This thesis proposes a stochastic ILS localizer receiver simulation model to estimate CDI output values given the power and frequencies of localizer signal and noise components. It is achieved by parametrizing each stage in an ILS receiver, including RF section, mixer, IF section, automatic gain control, IF envelope detector and 90/150 Hz detection stage. The nonlinear characteristics of RF amplifier, mixer and IF amplifier is approximated by a third-order polynomial. All receiver characteristics are parametrized, and the values of parameters are inverted by fitting simulation results with AAM, ITU and ICAO curves for a chosen test condition. The inverted receiver model could be verified from other test conditions. Simulation results fit empirical data well for three-frequency, pure-carrier and fifth-order intermodulation conditions. It is an indication that our generic model could capture the performance of ILS localizer receivers. For brute-force interference, simulation results indicate that intermodulation and AGC may not be the principal causes. Other nonlinear mechanism, such as clamping effect at front end, may take the responsibility for interference at high input noise level.

The purpose of this research is embedded in a broader scenario: the overall simulation of the aircraft landing process under the realistic radio environment. The combination of receiver model with aircraft aerodynamic model, aircraft control law model, EM propagation model and the database of the position, power, frequency of ILS localizer and FM stations offer a tool for the simulation of aircraft landing trajectory. The statistics obtained from Monte Carlo simulation on landing trajectories such as failure rate provides a clear reference of automatic landing system performance within a specific geographic region. A complete receiver is an indispensable part of the overall system evaluation model.

The ILS localizer receiver model is still far from comprehensive. Several issues are important for the achievement of a more accurate model in the future. Fifth-order intermodulation effect should be considered when input noise power is relatively higher than that at third-order threshold level. The immediate modification is replacing the transfer function of nonlinear amplifier, $y = K_1x + K_3x^3$, by $y = K_1x + K_3x^3 + K_5x^5$. And the fifth-order intermodulation is generated by the fifth-order harmonic K_5x^5 . But more complication is involved for the contribution of intermodulation power when more than one nonlinear stage are connected. It requires more theoretical and simulation works. In addition, intermodulation cannot explain the brute-force(B2) interference. It is generally believed that brute-force interference happens because the high noise power level desensitizes the receiver thus to change localizer output. It could result from AGC desensitization – the noise power leaks through IF filter therefore to drive AGC to reduce localizer amplitude, or from front-stage nonlinearity – the high noise power at front stages (e.g. RF section, mixer) drives the device into highly nonlinear region to distort baseband localizer signal. To understand the mechanism of brute-force interference further investigation is required, too.

Reference

- [1] Bennett, W. R., " Cross modulation requirements on multi-channel amplifiers below overload, " *Bell Syst. Tech. J.*, Vol. 19, pp. 587-610, 1940
- [2] Bose, K. W., *Aviation Electronics*, Indiana: Howard W. Sams & Co., Inc., 1981
- [3] CCIR Study Groups, *Compatibility between the sound broadcasting service in the band of about 87 -108 MHz and the aeronautical service in the band 108 -137 MHz*, CCIR Draft Recommendation [F/12], 1992
- [4] Chang, K. Y., " Intermodulation noise and products due to frequency dependent nonlinearities in CATV systems, " *IEEE Tran. on Comm.*, Vol. COM-23, No. 1, pp. 142-155, 1975
- [5] Chua, L. O., Desoer, C. A., Kuh, E. S., *Linear and nonlinear circuits*, New York: McGraw-Hill, 1987
- [6] Edwards, R., Durkin, J., Green, D.H., " Selection of intermodulation-free frequencies for multiple-channel mobile radio systems, " *Proc. IEEE*, Vol. 56, No. 12, pp. 862-870, 1968
- [7] Essman, J. E., Loos, T., *Analytical determination of the interference of commercial FM stations with airborne communication and navigation receivers and experimental verifications*, FAA technical report, FAA-R-6050-1, 1978

- [8] Evans, B. G., Ganem, H., "Simulation of FM/FDM blocks for interference and intermodulation calculations," *Electro. Letter*, Vol. 17, No. 25, pp. 963-964, 1981

- [9] Federal Aviation Administration, *User's manual and technical reference for the airspace analysis: mathematical model*, FAA Spectrum Engineering Division, ASM-500, Version 4.1, 1992.

- [10] Federal Aviation Administration, *Microwave landing system demonstration program, project summaries and MLS user financial analysis*, FAA project report, 1991

- [11] Gardiner, J. G., Magaza, M. S. A., "Some alternative frequency assignment procedure for mobile radio systems," *Radio and Electro. Eng.*, Vol. 52, No. 4, pp. 193-197, 1982

- [12] Gavan, J., Shulman, M. B., "Effect of desensitization on mobile radio system performance, part I: qualitative analysis," *IEEE Tran. on Vehicular Tech.*, Vol. VT-33, No. 4, pp. 285-290, 1984

- [13] Gavan, J., Shulman, M. B., "Effect of desensitization on mobile radio system performance, part II: quantitative analysis," *IEEE Tran. on Vehicular Tech.*, Vol. VT-33, No. 4, pp. 291-300, 1984

- [14] Gavan, J., "Main effect of mutual interference in radio communication systems using broad-band transmitters," *IEEE Tran. on EMC.*, Vol. EMC-28, No. 4, pp. 211-219, 1986

- [15] Jones, J. R., Jones, S. H., Tait, G. B., Zybur, M. F., " Heterostructure barrier varactor simulation using an integrated hydrodynamic device/harmonic-balance circuit analysis technique, " *IEEE Microwave and Guided Wave Letter*, Vol. 4, No. 12, pp. 411-413, 1994
- [16] Kavehrad, M., " Multiple FM/FDM carriers through nonlinear amplifiers, " *IEEE Tran. on Comm.*, Vol. COM-29, No. 5, pp. 751-756, 1981
- [17] Koh, P. J., Peatman, C. B., Crowe, T. W., " Millimeter wave tripler evaluation of a metal/2-deg Schottky diode varactor, " *IEEE Microwave and Guided Wave Letter*, Vol. 5, No. 2, pp. 73-75, 1995
- [18] Kuester, J. L., Mize, J. H., *Optimization techniques with Fortran*, 1973
- [19] Perlow, S. W., " Third-order distortion in amplifiers and mixers, " *RCA Review*, Vol. 37, pp. 234-266, 1976
- [20] Radiocommunication Study Groups, International Telecommunication Union (ITU), *Test procedures for measuring aeronautical receiver characteristics used for determining compatibility between the sound-broadcasting service in the band of about 87 -108 MHz and the aeronautical service in the band 108 -118 MHz*, Draft New Recommendation ITU-R [DOC.2/XX], 1995
- [21] Sedra, A. S., Smith, K. C., *Microelectronic circuits*, New York: Holt, Rinehart and Winston, 1982
- [22] Shen, Y. C., Tou, C. P., " A scheme for further strengthening interference protection of spread spectrum communication systems, " *1990 International Symp. on EMC, Symp. Record*, pp. 532-536. 1990

- [23] Simons, K. A., " The decibel relationships between amplifier distortion products, " *Proc. IEEE*, Vol. 56, No. 12, pp. 862-870, 1968
- [24] Stapleton, S. P., Quach, L., " Reduction of adjacent channel interference using postdistortion, " *42th Vehicular Tech. Soc. Conference, 1992*, Vol. 2, pp. 915-918, 1992
- [25] Steiner, J. W., " An analysis of radio frequency interference due to mixer intermodulation products, " *IEEE Tran. on EMC*, Vol. EMC-6, No. 1, pp. 62-68, 1964
- [26] The Analytic Science Corporation (TASC), *Description of ILS localizer receiver models and signal environment models*, Technical information memorandum, 1990
- [27] Wang, L. F., *Intermodulation analysis of receivers*, M.S. thesis, Dept. of Electrical Engineering and Computer Science, Massachusetts Institute of Technology, 1992
- [28] Wass, C. A. A., " A table of intermodulation products, " *IEE Journal*, Vol. 95, Part 3, pp. 31-39, 1948
- [29] Weiner, D. D., Spina, J. F., *Sinusoidal analysis and modeling of weakly nonlinear circuits*, Van Nostrand Reinhold, 1980

5220240